Stem Cell Reports
Article

ISSCR

OPEN ACCESS

# YAP signaling in horizontal basal cells promotes the regeneration of olfactory epithelium after injury

Qian Wu,[1,2,6] Xingxing Xu,[3,6] Xuemeng Miao,[1,2,6] Xiaomei Bao,[3] Xiuchun Li,[5] Ludan Xiang,[2] Wei Wang,[2] Siyu Du,[2] Yi Lu,[2] Xiwu Wang,[3] Danlu Yang,[3] Jingjing Zhang,[3] Xiya Shen,[3] Fayi Li,[5] Sheng Lu,[5] Yiren Fan,[2] Shujie Xu,[2] Zihao Chen,[2] Ying Wang,[1,4,*] Honglin Teng,[5,*] and Zhihui Huang[1,2,5,*]

[1]School of Pharmacy, Hangzhou Normal University, Hangzhou, Zhejiang 311121, China
[2]School of Mental Health, Wenzhou Medical University, Wenzhou, Zhejiang 325035, China
[3]School of Basic Medical Sciences, Wenzhou Medical University, Wenzhou, Zhejiang 325035, China
[4]Department of Transfusion Medicine, Zhejiang Provincial People's Hospital of Hangzhou Medical College, Hangzhou, Zhejiang 310053, China
[5]Department of Orthopedics (Spine Surgery), The First Affiliated Hospital of Wenzhou Medical University, Wenzhou, Zhejiang 325035, China
[6]These authors contributed equally
*Correspondence: nancywangying@163.com (Y.W.), honlinten@163.com (H.T.), huang0069@hznu.edu.cn (Z.H.)
https://doi.org/10.1016/j.stemcr.2022.01.007

## SUMMARY

The horizontal basal cells (HBCs) of olfactory epithelium (OE) serve as reservoirs for stem cells during OE regeneration, through proliferation and differentiation, which is important in recovery of olfactory function. However, the molecular mechanism of regulation of HBC proliferation and differentiation after injury remains unclear. Here, we found that yes-associated protein (YAP) was upregulated and activated in HBCs after OE injury. Deletion of YAP in HBCs led to impairment in OE regeneration and functional recovery of olfaction after injury. Mechanically, YAP was activated by S1P/S1PR2 signaling, thereby promoting the proliferation of HBCs and OE regeneration after injury. Finally, activation of YAP signaling enhanced the proliferation of HBCs and improved functional recovery of olfaction after OE injury or in Alzheimer's disease model mice. Taken together, these results reveal an S1P/S1PR2/YAP pathway in OE regeneration in response to injury, providing a promising therapeutic strategy for OE injury.

## INTRODUCTION

The adult mammalian olfactory epithelium (OE) has long been known for its unique characteristic of actively generating neurons throughout life from basal stem cells (Choi and Goldstein, 2018; Schwob et al., 2017). Olfactory sensory neurons (OSNs) in the nasal cavity are highly vulnerable to the insults of external environments such as inspired chemicals, toxins, and viruses including SARS-Cov-2 (Zhang et al., 2021). Basal stem cells in the basal layer of OE, including horizontal basal cells (HBCs) and globose basal cells (GBCs), possess robust regenerative ability to replenish injury-induced loss of OSNs. HBCs are mitotically quiescent under physiological conditions but activated after severe OE injury (Iwai et al., 2008; Leung et al., 2007; Schwob et al., 1995), whereas GBCs are mitotically active and responsible for OE regeneration under most conditions (Huard and Schwob, 1995). Under OE injury, such as exposure to methyl bromide or ablation with methimazole, HBCs act as stem cells and can be activated to facilitate differentiation, proliferation, and migration of OE cells during regeneration (Herrick et al., 2017; Joiner et al., 2015; Schnittke et al., 2015). HBCs are marked by the expression of p63, keratin5/14 (K5/14), and intercellular adhesion molecule 1 (Carter et al., 2004; Fletcher et al., 2011; Holbrook et al., 1995), and *in vitro* experiments have shown that they have multipotent potential to generate diverse cell types of OE (Carter et al., 2004). Recent studies have further demonstrated that engrafted HBCs produce all OE cell types, confirming HBC's multipotency (Peterson et al., 2019). However, the regenerative potential of OE is diminished during aging, leading to anosmia in some diseases, such as Alzheimer's disease (AD) (Attems et al., 2015; Doty, 2018). Although recent studies based on genetic strategies have shown that transcription factors such as p63 (Fletcher et al., 2011; Schnittke et al., 2015), Wnt signaling (Chen et al., 2014; Fletcher et al., 2017), Notch signaling (Herrick et al., 2017), and inflammation signaling (Chen et al., 2017, 2019) contribute to OE regeneration after injury, the mechanism underlying the proliferation and differentiation of these basal stem cells in OE response to injury is complex and not fully understood.

Yes-associated protein (YAP) and its paralog, the transcriptional co-activator with PDZ-binding motif (TAZ), which is also known as WW-domain-containing transcription regulator 1 (WWTR1), act as transcriptional co-activators and well-known downstream effectors of the highly conserved Hippo pathway, are expressed in the stem/progenitor cells of vertebrate tissues, and control cell proliferation, tissue homeostasis, and organ size (Andl et al., 2017; Elbediwy and Thompson, 2018; Moya and Halder, 2019; Rognoni and Walko, 2019). Activation of YAP signaling has been shown to promote the proliferation of epidermal stem cells and progenitor cells (Rognoni and Walko, 2019; Schlegelmilch et al., 2011), whereas YAP deletion in K14-expressing mice led to fewer stem cells within the epidermis,

fewer hair follicles, and faster death due to failure of the epidermal barrier, indicating the essential role of YAP in skin stem cell regeneration (Elbediwy and Thompson, 2018; Rognoni and Walko, 2019; Schlegelmilch et al., 2011). Moreover, YAP is highly expressed and required for the self-renewal of cultured embryonic stem cells as well as the suppression of differentiation (Lian et al., 2010). However, existing evidence also shows that knockdown of YAP and TAZ in the skin of mice by small interfering RNA does not affect the development and function of the skin (Lee et al., 2014). In addition, YAP knockout in neural stem cells (NSCs) is not required for their proliferation (Huang et al., 2016). Interestingly, the S1PR1/RhoA/YAP pathway promotes the proliferation of olfactory ensheathing cells, and is involved in development of the olfactory nerve layer, and growth and axonal projection of olfactory neurons into the olfactory bulb (OB) (Bao et al., 2020). However, it is still largely unclear whether YAP signaling is involved in OE regeneration after injury.

In the present study, we found that YAP deletion in HBCs impaired OE regeneration and olfactory functional recovery in the methimazole-induced OE injury model. Moreover, sphingosine 1-phosphate (S1P) activated YAP and promoted the proliferation of HBCs and OE regeneration after injury. Finally, activation of YAP signaling enhanced the proliferation of HBCs and improved functional recovery of the olfactory system after injury or in AD model mice. Therefore, this study provides novel insights into the mechanism of OE regeneration, providing a promising therapeutic strategy for OE injury.

## RESULTS

### YAP is upregulated and activated in the HBCs of OE after acute injury

To explore the potential effects of YAP on OE regeneration after injury, we performed double immunostaining, which showed that YAP was highly expressed in $p63^+$ (a marker of HBCs) cells of adult OE (Figure 1A), but not or very lowly expressed in $LSD1^+$ cells (a marker of GBCs) (Figure 1B), $GAP43^+$ cells (a marker of immature olfactory sensory neurons [iOSNs]) (Figure 1C), and $OMP^+$ cells (a marker of mature olfactory sensory neurons [mOSNs]) (Figure 1D). These results suggest that YAP is mainly expressed in HBCs.

A methimazole-induced OE injury model was used to test the function of YAP in HBCs. Consistent with a previous study (Ogawa et al., 2014), administration of methimazole caused the death of OE cells within 24 h and OE was gradually recovered within 4 weeks after injury (Figures S1A and S1B). Moreover, the buried pellet behavioral assay revealed that methimazole indeed impaired the olfactory function (Figures S1C and S1E).

Based on this model, western blot results showed that YAP was significantly upregulated from 3 days post lesion (dpl) (Figures 1E and 1G), while the p-YAP/YAP ratio was decreased from 3 dpl (Figures 1E and 1F). Interestingly, TAZ/WWTR1 was significantly upregulated after OE injury from 3 dpl (Figures 1H and 1I), indicating that TAZ might also be activated in OE after injury. Immunohistochemistry also showed that YAP was significantly increased in a time-dependent manner from 0 to 14 dpl (Figures 1J and 1K). Additionally, co-immunostaining analysis found that YAP was significantly increased and displayed the nuclear location in HBCs from 1 dpl (Figures 1L and 1M). Taken together, these results suggest that YAP is upregulated and activated in HBCs after acute OE injury.

### Normal development of OE and olfactory function in $YAP^{K5}$-CKO mice

$YAP^{K5}$-CKO mice were generated by crossing the $YAP^{f/f}$ with K5-Cre transgenic mice (Figures S2A and S2B). YAP was indeed efficiently knocked out in $p63^+$ and $K5^+$ (a marker of HBCs) cells of $YAP^{K5}$-CKO mice (Figures S2C and S2D). However, there was no significant difference in body weight between $YAP^{f/f}$ and $YAP^{K5}$-CKO mice during development (Figure S2E). Furthermore, YAP deletion in $K5^+$ cells also did not affect the development of skin (Figures S2F and S2G). Consequently, H&E staining showed that the morphology and thickness of OE were comparable between the $YAP^{f/f}$ and $YAP^{K5}$-CKO mice (Figure S3A). The buried pellet test revealed that there was no significant difference between $YAP^{f/f}$ and $YAP^{K5}$-CKO mice in the percentage of mice that found food in allotted time (Figure S3B) and the time taken to find food (Figure S3C). Moreover, YAP deletion in HBCs also did not affect the distribution and number of HBCs (Figures S3D and S3E), $GAP43^+$ iOSNs (Figure S3F), $OMP^+$ mOSNs (Figure S3G), and $Sox9^+$ cells (a marker of Bowman's gland duct cells) (Figure S3H). These results suggest that YAP deletion in HBCs does not affect the development of OE and olfactory function.

### YAP deletion in HBCs impairs OE regeneration and functional recovery of the olfactory system after injury

As shown in Figures 2A and 2B, OE gradually regenerated in $YAP^{f/f}$ mice after injury and almost recovered at 28 dpl. However, OE failed to completely recover in $YAP^{K5}$-CKO mice within 28 days after injury. Moreover, the buried pellet test showed that the percentage of mice that found food was significantly decreased (Figure 2C), and the time consumed to find food was markedly prolonged in $YAP^{K5}$-CKO mice from 14 to 28 dpl (Figure 2D). These results suggest that YAP deletion in HBCs impairs OE regeneration and functional recovery of the olfactory system after injury.

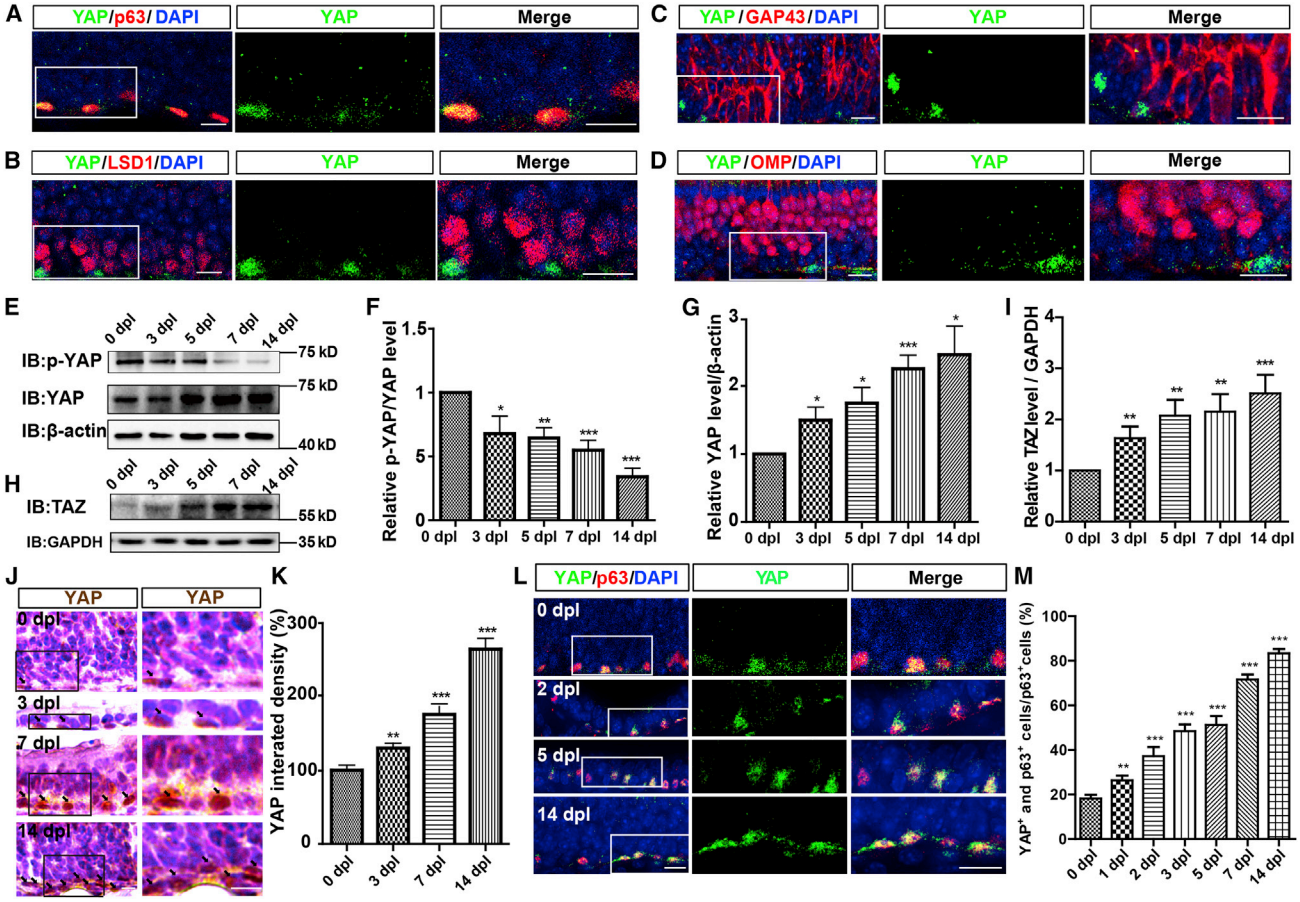


**Figure 1. YAP is upregulated and activated in HBCs after acute OE injury**

(A–D) Double immunostaining of YAP (green) and p63 (red) (A), YAP (green) and LSD1 (red) (B), YAP (green) and GAP43 (red) (C), and YAP (green) and OMP (red) (D) in the OE of 2-month-old C57BL/6 mice.

(E) Western blot detected the expression of p-YAP and YAP in the OE of 2-month-old C57BL/6 mice at 0, 3, 5, 7, and 14 dpl.

(F and G) Quantitative analysis of the relative p-YAP/YAP (F) and YAP (G) levels as shown in (E) (n = 8 blots from 4 mice per group, normalized to the 0 dpl group).

(H) Western blot detected the expression of TAZ in the OE of 2-month-old C57BL/6 mice at 0, 3, 5, 7, and 14 dpl.

(I) Quantitative analysis of the relative TAZ level as shown in (H) (n = 15 blots from 5 mice per group, normalized to the 0 dpl group).

(J) Immunohistochemistry detected the expression of YAP in the OE of 2-month-old C57BL/6 mice at 0, 3, 7, and 14 dpl.

(K) Quantitative analysis of the relative YAP density as shown in (J) (n = 10 sections from 5 mice per group).

(L) Double immunostaining of YAP (green) and p63 (red) in the OE of 2-month-old C57BL/6 mice at 0, 2, 5, and 14 dpl.

(M) Quantitative analysis of the percentage of both $YAP^+$ and $p63^+$ cells over $p63^+$ cells as shown in (L) (n = 9 sections from 3 mice per group).

Images of selected regions are shown at higher magnification. Data are mean ± SEM, one-way ANOVA with Bonferroni's post tests, compared with 0 dpl group; *p < 0.05, **p < 0.01, ***p < 0.001. Scale bars, 20 μm.

## YAP deletion in HBCs reduces their proliferation and the regeneration of OSNs and inhibits axonal projection of OSNs into OB after injury

Given that YAP is involved in self-renewal of stem cells (Yao et al., 2014), the proliferation of HBCs was examined after injury in both $YAP^{f/f}$ and $YAP^{K5}$-CKO mice. As expected, double immunostaining showed that the percentage of $Ki67^+$ or $PH3^+$ (markers of cell proliferation) cells was significantly decreased in HBCs of $YAP^{K5}$-CKO mice from 1 dpl to 5 dpl (Figures 3A and 3D). However, TUNEL staining showed that there was no significant difference in the apoptosis of HBCs after injury between $YAP^{f/f}$ and $YAP^{K5}$-CKO mice (Figures 3E and 3F). These results indicate that YAP deletion in HBCs reduces their proliferation after injury.

To further investigate whether YAP deletion in HBCs affected their differentiation after OE injury, we conducted

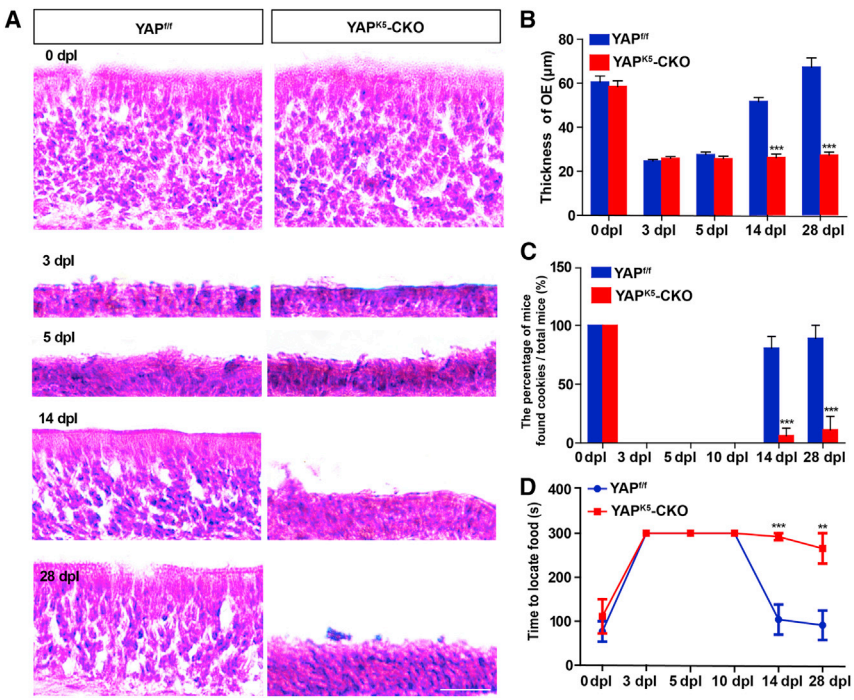


**Figure 2. YAP deletion in HBCs impairs OE regeneration and functional recovery of the olfactory system after injury**

(A) H&E staining of the OE obtained from 2-month-old $YAP^{f/f}$ and $YAP^{K5}$-CKO mice at 0, 3, 5, 14, and 28 dpl.

(B) Quantitative analysis of the thickness of OE as shown in (A) (n = 10 sections from 5 mice per group).

(C) Percentage of mice that found cookies over total observed 2-month-old $YAP^{f/f}$ (n = 9 mice) or $YAP^{K5}$-CKO mice (n = 10 mice) in the buried pellet test at 0, 3, 5, 10, 14, and 28 dpl.

(D) Quantitative analysis of the time to locate food of 2-month-old $YAP^{f/f}$ (n = 9 mice) and $YAP^{K5}$-CKO mice (n = 10 mice) at 0, 3, 5, 10, 14, and 28 dpl in the buried pellet test.

Data are mean ± SEM, two-way ANOVA with Bonferroni's post tests, compared with $YAP^{f/f}$ group; **p < 0.01, ***p < 0.001. Scale bars, 20 μm.

immunostaining, which revealed a significant decrease in the number of $GAP43^+$ iOSNs in the $YAP^{K5}$-CKO mice from 7 dpl to 28 dpl (Figures 4A and 4B). Moreover, the number of $OMP^+$ mOSNs was also significantly reduced in $YAP^{K5}$-CKO mice from 14 dpl to 28 dpl (Figures 4A and 4C). However, the number of $Sox9^+$ Bowman's gland duct cells was not affected in the $YAP^{K5}$-CKO mice at 14 dpl (Figures 4D and 4E). These results suggest that YAP deletion in HBCs reduces the number of OSNs after OE injury, probably due to reduction of HBC proliferation.

To examine the effects of YAP in HBCs on the axonal projections to the glomeruli of newly generated OSNs, we measured the OMP-positive areas within individual glomeruli of OB at 0, 7, and 14 dpl. Previous studies have shown that the OMP-positive area within the individual glomeruli in OB decreases at 7 and 14 dpl, probably due to the clearance of the degenerative olfactory axons after injury (Kikuta et al., 2015). Consistently, the positive area of OMP signal in OB decreased at 7 and 14 days after injury (Figures 4F and 4G), and the decrease was more significantly in $YAP^{K5}$-CKO mice (Figures 4F and 4G). These results therefore suggest that YAP deletion in HBCs results in less projection of axons from newly generated OSNs.

## The upstream signaling molecule S1PR2 is expressed in HBCs and activates YAP in OE after injury

Given that S1P, being upstream of YAP, plays a prominent role in cell proliferation (Cheng et al., 2018; Liu et al., 2018; Yu et al., 2016), to explore whether S1P/YAP signaling enhances OE regeneration, S1P was applied to the methimazole-treated $YAP^{f/f}$ and $YAP^{K5}$-CKO mice. Although S1P treatment did not improve functional recovery of the olfactory system (Figure 5A), it indeed accelerated OE regeneration of $YAP^{f/f}$ mice; however, it failed to promote OE regeneration of $YAP^{K5}$-CKO mice (Figures 5B and 5C). Furthermore, S1P treatment promoted the proliferation of HBCs in $YAP^{f/f}$ mice but not in $YAP^{K5}$-CKO mice at 1 dpl and 2 dpl (Figures 5D and 5E). Additionally, there was a significant increase in $GAP43^+$ iOSNs and $OMP^+$ mOSNs after S1P treatment at 14 dpl in $YAP^{f/f}$ mice but not in $YAP^{K5}$-CKO mice (Figures 5F–5I).

Double immunostaining further showed that S1PR1 was not expressed in HBCs but in lamina propria (LP) (Figure S4A); however, S1PR2 was mainly expressed in HBCs (Figure S4B). Additionally, the expression of S1PR2 in HBCs was significantly increased from 3 dpl to 14 dpl (Figures S4C and S4D), and the expression pattern of S1PR2 in HBCs after injury was similar to that of YAP, indicating that S1PR2 might be an upstream molecule of YAP signaling (Figure S4E).

Moreover, the levels of YAP in HBCs as well as $YAP^+$ HBCs were reduced after JTE013 (an antagonist of S1PR2) treatment from 5 dpl to 14 dpl (Figures S4F–S4I). In addition, OE became significantly thinner after treatment with JTE013 at 14 dpl (Figures 6A and 6B). The buried pellet test showed that JTE013 treatment significantly increased the possibility of failure (Figure 6C) and prolonged the time taken to find food at 14 dpl (Figure 6D). Furthermore,

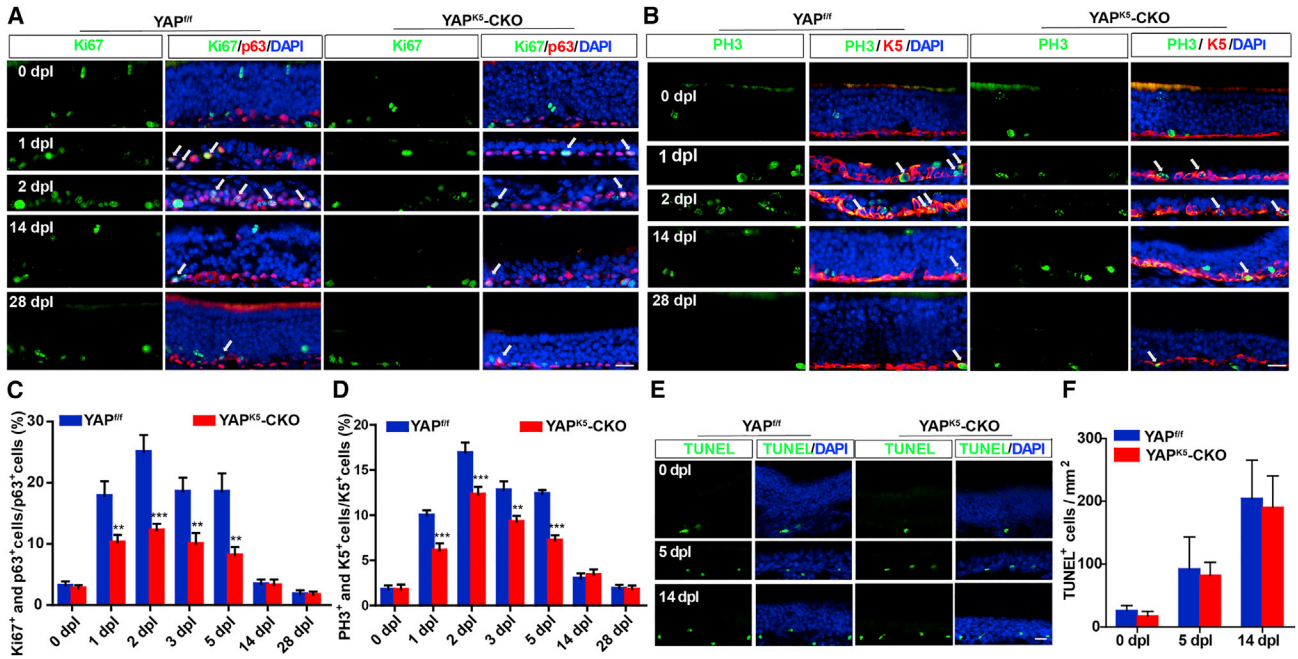


**Figure 3. YAP deletion in HBCs reduces the proliferation of HBCs in OE after injury**

(A and B) Double immunostaining of Ki67 (green) and p63 (red) (A) or PH3 (green) and K5 (red) (B) in the OE of 2-month-old $YAP^{f/f}$ and $YAP^{K5}$-CKO mice at 0, 1, 2, 14, and 28 dpl.

(C and D) Quantitative analysis of the percentage of $Ki67^+$ and $p63^+$ cells over total $p63^+$ cells (C), or $PH3^+$ and $K5^+$ cells over total $K5^+$ cells (D) in the OE of 2-month-old $YAP^{f/f}$ and $YAP^{K5}$-CKO mice at 0, 1, 2, 3, 5, 14, and 28 dpl as shown in (A) and (B) (n = 10 sections from 5 mice per group).

(E) Cell apoptosis detected by TUNEL staining in the OE of 2-month-old $YAP^{f/f}$ and $YAP^{K5}$-CKO mice at 0, 5, and 14 dpl.

(F) Quantitative analysis of the density of $TUNEL^+$ cells as shown in (E) (n = 15 sections from 5 mice per group).

Data are mean ± SEM, two-way ANOVA with Bonferroni's post tests, compared with $YAP^{f/f}$ group; $^{**}p < 0.01$, $^{***}p < 0.001$. Scale bars, 20 μm.

the percentage of $Ki67^+$ or $PH3^+$ cells in HBCs was reduced after JTE013 treatment at 3 dpl and 5 dpl (Figures 6E–6H). There was a significant reduction in the number of $GAP43^+$ iOSNs after JTE013 treatment at 7 dpl to 14 dpl (Figures 6I and 6J). Moreover, the number of $OMP^+$ mOSNs was also significantly reduced in the JTE013 group at 14 dpl (Figures 6I and 6K). These results suggest that S1P/S1PR2/YAP signaling promotes HBC proliferation and OE regeneration after injury.

## Activation of YAP promotes HBC proliferation, OE regeneration, and functional recovery of the olfactory system after acute injury or in AD model mice

To test whether activation of YAP signaling promotes OE regeneration after injury, we applied XMU-MP-1, an inhibitor of MST1 and MST2. As expected, XMU-MP-1 treatment indeed significantly activated YAP in HBCs at 3 dpl and 7 dpl (Figures 7A–7C and 7F), and decreased the p-MOB1/MOB1 and p-YAP/YAP ratio (Figures 7C–7E). Interestingly, XMU-MP-1 treatment increased the thickness of OE (Figures 7G and 7H) and promoted functional recovery of the olfactory system at 7 dpl (Figure 7I). Furthermore, the proliferation of HBCs was increased at 3 dpl by XMU-MP-1 treatment (Figures 7J–7M). The number of $GAP43^+$ OSNs was significantly increased at 7 dpl by XMU-MP-1 treatment (Figures 7N and 7O). These results suggest that YAP activation promotes OE regeneration and functional recovery of the olfactory system after acute injury.

Recent studies have shown that Aβ appears in OE after 1–2 months of age, coinciding with the degeneration of OSNs in AD model mice and patients as well as rapid decrease in the OE thickness (Bahar-Fuchs et al., 2010; Wu et al., 2013; Yoo et al., 2017). To explore the therapeutic effect of YAP on olfactory dysfunction in AD, we used APP/PS1 model mice. Thioflavin-S staining revealed a widespread distribution of Aβ plaques in cortex and hippocampus of AD model mice (Figure S5A). Interestingly, there was a significant decrease in YAP expression of AD model mice (Figures S5B and S5C). The buried pellet test also showed that, to a certain extent, the olfactory function of these mice was improved (Figure S5D). Furthermore, XMU-MP-1 treatment promoted the proliferation of HBCs (Figures S5E and S5F) and the

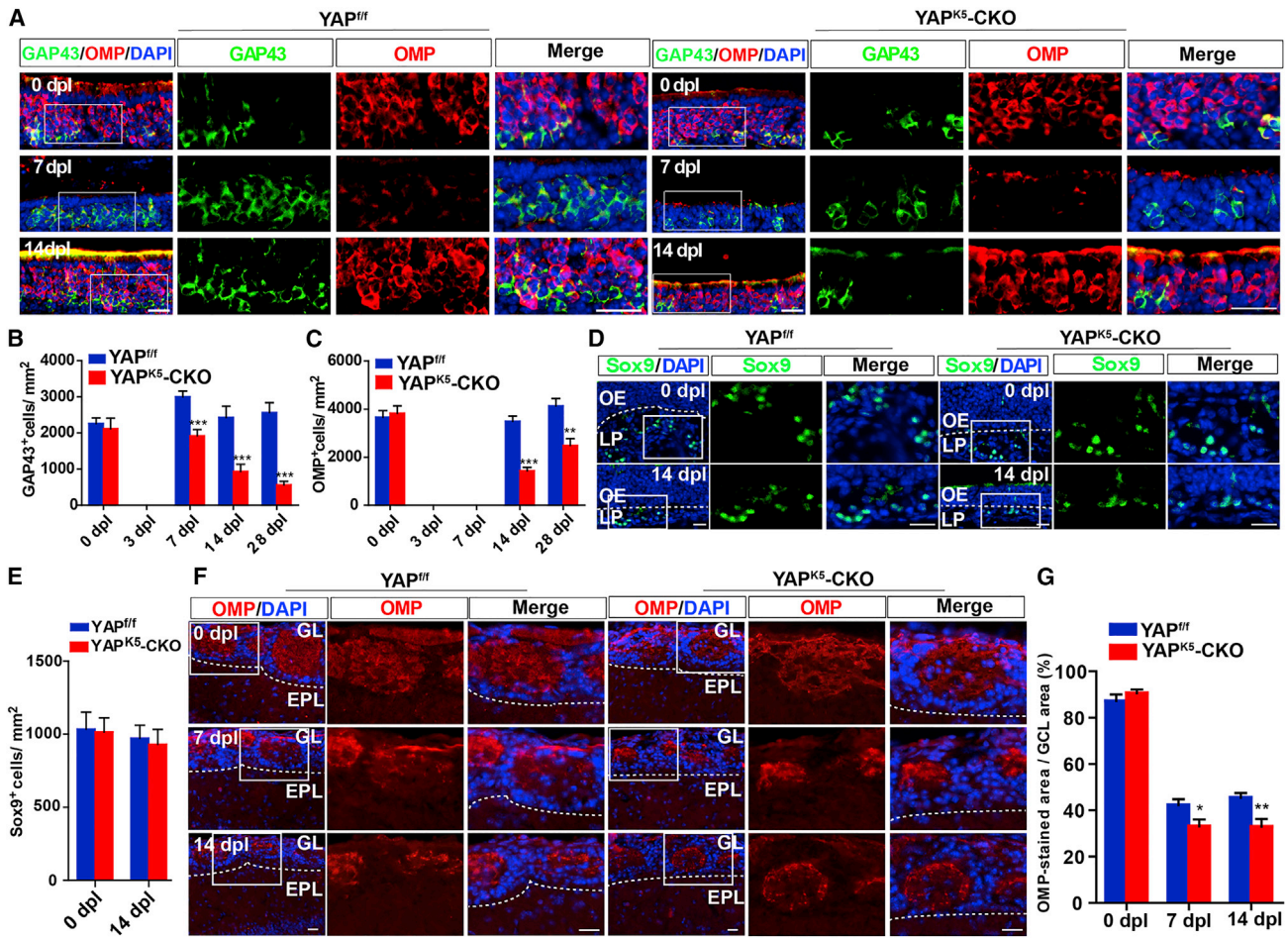


**Figure 4. YAP deletion in HBCs reduces the regeneration of OSNs after OE injury**

(A) Double immunostaining of GAP43 (green) and OMP (red) in the OE of 2-month-old YAP$^{f/f}$ and YAP$^{K5}$-CKO mice at 0, 7, and 14 dpl.

(B and C) Quantitative analysis of the density of GAP43$^{+}$ (B) or OMP$^{+}$ (C) cells in the OE of 2-month-old YAP$^{f/f}$ and YAP$^{K5}$-CKO mice at 0, 3, 7, 14, and 28 dpl (n = 9 sections from 5 mice per group).

(D) Immunostaining of Sox9 (green) in the OE of 2-month-old YAP$^{f/f}$ and YAP$^{K5}$-CKO mice at 0 and 14 dpl.

(E) Quantitative analysis of the density of Sox9$^{+}$ cells as shown in (D) (n = 11 sections from 5 mice per group).

(F) Immunostaining of OMP (red) in the OB of 2-month-old YAP$^{f/f}$ and YAP$^{K5}$-CKO mice at 0, 7, and 14 dpl. EPL, external plexiform layer; GL, glomerular layer.

(G) Quantitative analysis of the percentage of area that showed OMP$^{+}$ area over granule cell layer (GCL) area as shown in (F) (n = 11 sections from 5 mice per group).

Images of selected regions are shown at higher magnification. Data are mean ± SEM, two-way ANOVA with Bonferroni's post tests, compared with YAP$^{f/f}$ group; *p < 0.05, **p < 0.01, ***p < 0.001. Scale bars, 20 μm.

regeneration of GAP43$^{+}$ iOSNs and OMP$^{+}$ mOSNs (Figures S5G–S5I) in AD model mice. These results suggest that YAP activation is sufficient to induce the proliferation of HBCs, promote OE regeneration, and improve functional recovery of the olfactory system in AD model mice.

## DISCUSSION

In this study, our findings reveal that YAP in HBCs is not required for development of the olfactory system. However, after OE injury, the S1P/S1PR2/YAP signaling triggers OE regeneration and improves functional recovery of the olfactory system by promoting the proliferation and differentiation of HBCs (Figure S6).

YAP signaling controls the regeneration of tissues, especially those characterized by rapid regeneration and renewal capability (Mendoza-Reinoso and Beverdam, 2018), such as the epidermis. In addition, previous studies showed that the distribution of YAP in epidermal tissue is similar to that of keratin, suggesting that YAP is mainly

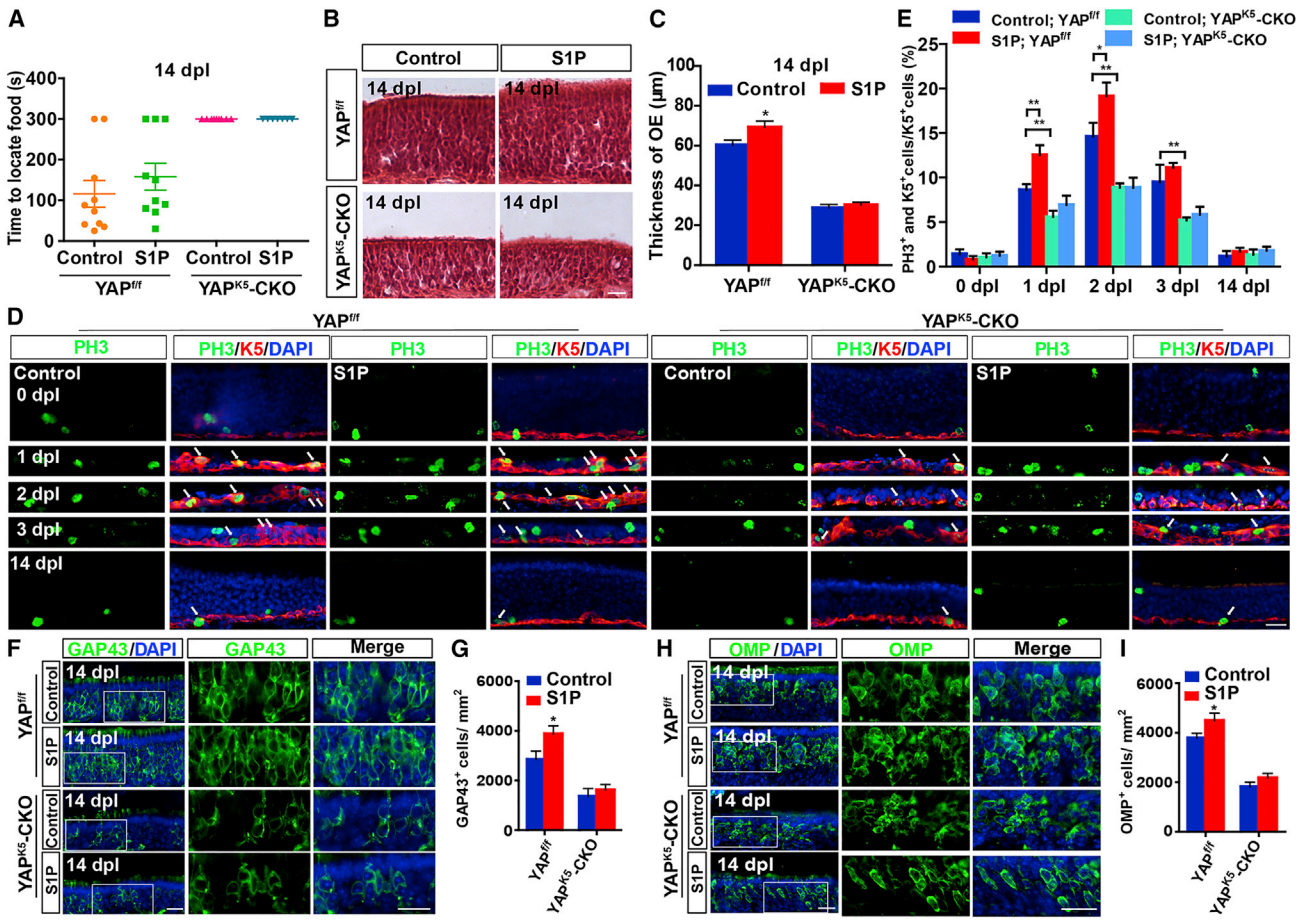


**Figure 5. S1P promotes OE regeneration after injury through YAP signaling**

(A) Quantitative analysis of the time to locate food in the buried pellet test in control-treated YAP$^{f/f}$ (n = 10 mice), S1P-treated YAP$^{f/f}$ (n = 10 mice), control-treated YAP$^{K5}$-CKO (n = 10 mice), and S1P-treated YAP$^{K5}$-CKO 2-month-old mice (n = 7 mice).

(B) H&E staining of the OE of control-treated 2-month-old YAP$^{f/f}$ and YAP$^{K5}$-CKO mice and S1P-treated 2-month-old YAP$^{f/f}$ and YAP$^{K5}$-CKO mice.

(C) Quantitative analysis of the thickness of OE as shown in (B) (n = 10 sections from 5 mice per group).

(D) Double immunostaining of PH3 (green) and K5 (red) in the OE of control-treated 2-month-old YAP$^{f/f}$ and YAP$^{K5}$-CKO mice and S1P-treated 2-month-old YAP$^{f/f}$ and YAP$^{K5}$-CKO mice at 0, 1, 2, 3, and 14 dpl.

(E) Quantitative analysis of the percentage of both PH3$^+$ and K5$^+$ cells over K5$^+$ HBCs as shown in (D) (n = 10 sections from 5 mice per group).

(F and H) Immunostaining of GAP43 (green) (F) or OMP (green) (H) in the OE of control-treated 2-month-old YAP$^{f/f}$ and YAP$^{K5}$-CKO mice and S1P-treated 2-month-old YAP$^{f/f}$ and YAP$^{K5}$-CKO mice at 14 dpl.

(G and I) Quantitative analysis of the density of GAP43$^+$ cells (G) or OMP$^+$ cells (I) per mm$^2$ as shown in (F) and (H) (n = 8 sections from 5 mice per group).

Images of selected regions are shown at higher magnification. Data are mean ± SEM, two-way ANOVA with Bonferroni's post tests, compared with control group; *p < 0.05, **p < 0.01. Scale bars, 20 μm.

distributed in the basal cells of the epidermis (Akladios et al., 2017). Similarly, the present study showed that YAP was highly expressed in the HBCs of OE but not in OSNs and GBCs (Figure 1). Additionally, YAP knockout in the HBCs had no effect on the development of OE and olfactory functions (Figure S3). These results were consistent with those from previous studies, which have shown that YAP knockout in stem cells did not affect the proliferation of NSCs (Huang et al., 2016), pancreatic stem cells (Zhang et al., 2014), and small intestinal stem cells (Azzolin et al., 2014). However, several other studies have shown that YAP is necessary for the regeneration of epithelial stem cells after injury (Hageman et al., 2020). In mouse epidermal basal cells, YAP has been shown to play a key

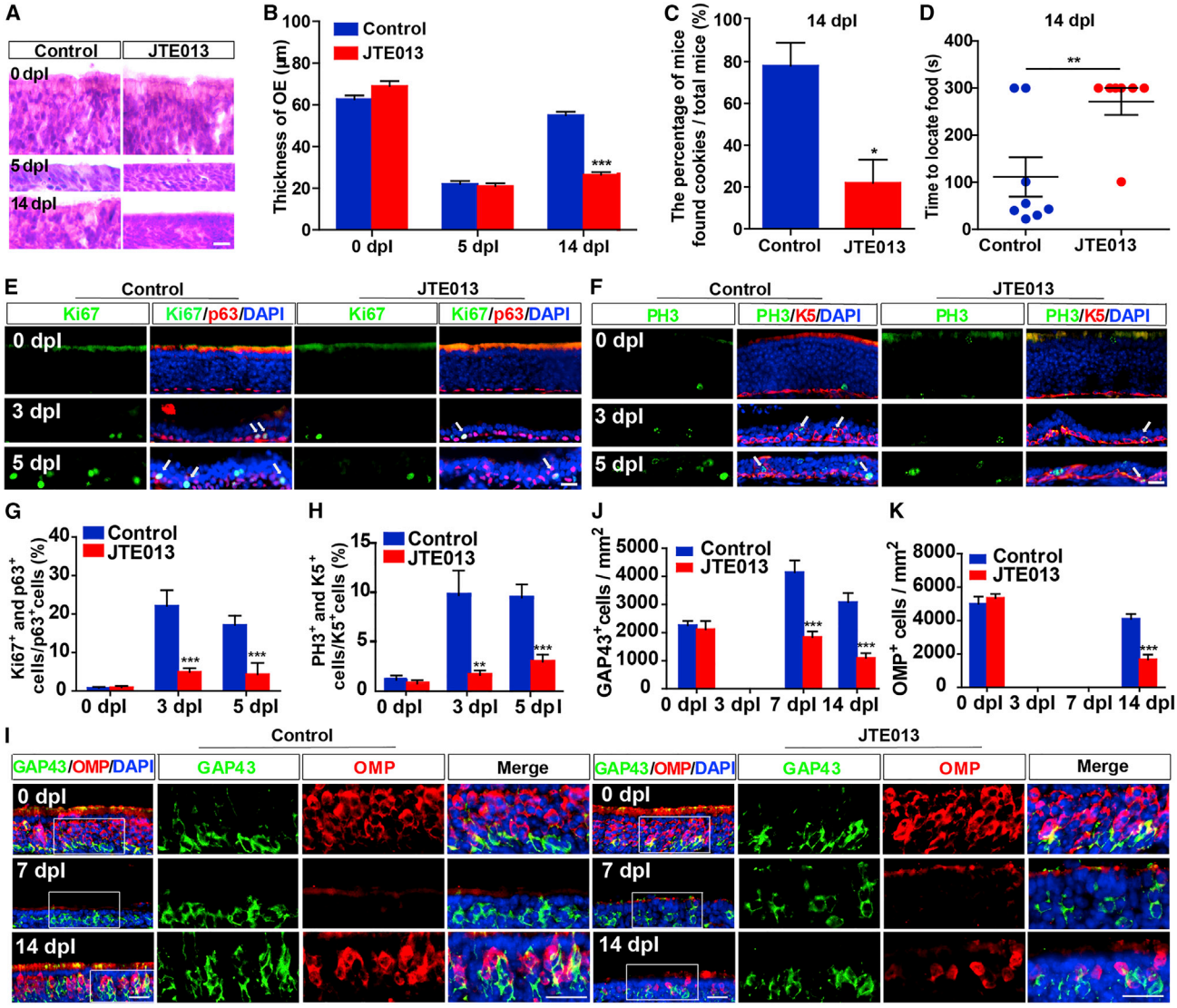


**Figure 6. Inhibition of S1PR2 impairs OE regeneration and functional recovery of the olfactory system after injury**

(A) H&E staining of the OE obtained from control- and JTE013-treated 2-month-old C57BL/6 mice at 0, 5, and 14 dpl.

(B) Quantitative analysis of the thickness of OE as shown in (A) (n = 7 sections from 4 mice per group).

(C) Percentage of mice that found cookies over total observed control-treated (n = 8 mice) or JTE013-treated 2-month-old C57BL/6 mice (n = 7 mice) in the buried pellet test at 14 dpl (Student's t test).

(D) Quantitative analysis of the time to locate food in control-treated (n = 8 mice) or JTE013-treated 2-month-old C57BL/6 mice (n = 7 mice) at 14 dpl in the buried pellet test (Student's t test).

(E and F) Double immunostaining of Ki67 (green) and p63 (red) (E) or PH3 (green) and K5 (red) (F) in the OE of control- and JTE013-treated 2-month-old C57BL/6 mice at 0, 3, and 5 dpl.

(G and H) Quantitative analysis of the percentage of both $Ki67^+$ and $p63^+$ cells (G) or $PH3^+$ and $K5^+$ (H) cells over $p63^+$ or $K5^+$ HBCs as shown in (E) and (F) (n = 10 sections from 4 mice per group).

(I) Double immunostaining of GAP43 (green) and OMP (red) in the OE of control- and JTE013-treated 2-month-old C57BL/6 mice at 0, 7, and 14 dpl.

(J and K) Quantitative analysis of the density of $GAP43^+$ (J) or $OMP^+$ (K) cells at 0, 3, 7, and 14 dpl (n = 6 sections from 4 mice per group). Images of selected regions are shown at higher magnification. Data are mean ± SEM, two-way ANOVA with Bonferroni's post tests unless otherwise indicated, compared with control group; *p < 0.05, **p < 0.01, ***p < 0.001. Scale bars, 20 μm.

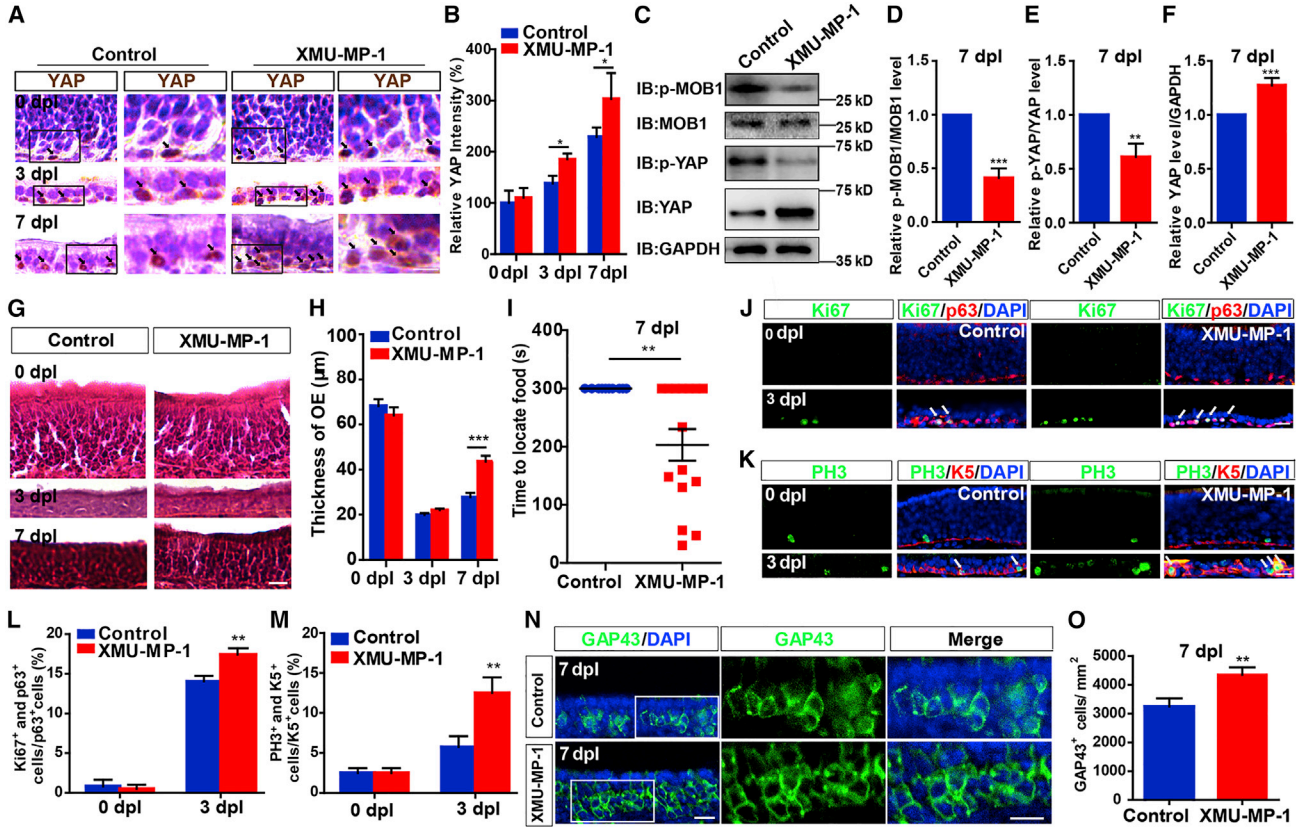


**Figure 7. Activation of YAP signaling by XMU-MP-1 promotes OE regeneration and functional recovery of the olfactory system after injury**

(A) Immunohistochemistry detected the expression of YAP in the OE of control- and XMU-MP-1-treated 2-month-old C57BL/6 mice at 0, 3, and 7 dpl.

(B) Quantitative analysis of the relative YAP density as shown in (A) (n = 6 sections from 6 mice per group).

(C) Western blot detected the expression of p-MOB1, MOB1, p-YAP, and YAP in OE of control- and XMU-MP-1-treated 2-month-old C57BL/6 mice at 7 dpl.

(D and F) Quantitative analysis of the relative p-MOB1/MOB1 (D), p-YAP/YAP (E), and YAP (F) levels as shown in (C) (normalized with control group, n = 8 blots from 4 mice per group, Student's t test).

(G) H&E staining of the OE obtained from control- and XMU-MP-1-treated 2-month-old C57BL/6 mice at 0, 3, and 7 dpl.

(H) Quantitative analysis of the thickness of OE as shown in (G) (n = 12 sections from 6 mice per group).

(I) Quantitative analysis of the time to locate food of control-treated (n = 10 mice) and XMU-MP-1-treated 2-month-old C57BL/6 mice (n = 13 mice) in the buried pellet test at 7 dpl (Student's t test).

(J and K) Double immunostaining of Ki67 (green) and p63 (red) (J) or PH3 (green) and K5 (red) (K) in the OE of control- and XMU-MP-1-treated 2-month-old C57BL/6 mice at 0 and 3 dpl.

(L and M) Quantitative analysis of the percentage of both $Ki67^+$ and $p63^+$ (L) or $PH3^+$ and $K5^+$ (M) cells over $p63^+$ or $K5^+$ HBCs as shown in (J) and (K) (n = 13 sections from 6 mice per group).

(N) Immunostaining of GAP43 (green) in the OE of control- and XMU-MP-1-treated 2-month-old C57BL/6 mice at 7 dpl.

(O) Quantitative analysis of the density of $GAP43^+$ cells as shown in (N) (n = 12 sections from 6 mice per group, Student's t test).

Images of selected regions are shown at higher magnification. Data are mean ± SEM, two-way ANOVA with Bonferroni's post tests unless otherwise indicated, compared with control group; *p < 0.05, **p < 0.01, ***p < 0.001. Scale bars, 20 μm.

role in the formation of a positive feedback loop with the epidermal growth factor receptor to promote the proliferation of basal stem cells after injury (Elbediwy et al., 2016). Additionally, YAP in the stem cells of the small intestine has been reported to be involved in intestinal regeneration after drug- or irradiation-induced injury (Gregorieff et al., 2015; Taniguchi et al., 2015). Furthermore, previous studies have shown that TAZ/WWTR1 is also important for stem/progenitor cell functions, and loss of either YAP or TAZ individually had no visible phenotype, confirming that

the two proteins act in a redundant fashion in this tissue (Elbediwy et al., 2016). Consistently, our studies also showed that YAP and TAZ were both significantly upregulated in OE after injury (Figure 1), indicating that YAP and TAZ might be important in OE after injury. Additionally, we found that the deletion of YAP in HBCs reduced their proliferation (Figure 3) and impaired the recovery of olfactory function (Figure 2) in the methimazole-induced OE injury model. These results indicate that YAP signaling in HBCs is required for OE regeneration after injury.

S1P is a sphingolipid metabolite with a wide range of biological activities and mainly secretes lipid mediators in the extracellular environment (Yu et al., 2012). S1PRs/YAP signaling plays an important role in various physiological and pathological conditions (Liu et al., 2018; Yu et al., 2012). In this study, S1PR1 was shown to be expressed in the LP but not in OE. S1PR2 was mainly expressed in HBCs and significantly upregulated in HBCs after injury (Figure S4). Moreover, treatment with JTE013 significantly inhibited the expression of YAP in HBCs (Figure S4), and attenuated the proliferation of HBCs and the regeneration of OSNs, thereby delaying regeneration of OE and the recovery (Figure 6). Notably, S1P was also shown to be generated in both blood and endothelial cells (Tukijan et al., 2018), which can release S1P into the circulation. Therefore, it is possible that after OE injury, the injured sites and/or the surrounding tissues such as blood vessels release S1P. Interestingly, although the exogenous application of S1P did not significantly improve the olfactory function recovery after injury (Figure 5), it indeed accelerated the regeneration of OE in the $YAP^{f/f}$ group; however, S1P failed to promote regeneration of OE in $YAP^{K5}$-CKO mice (Figure 5). Taken together, our results show that S1P/S1PR2/YAP signaling promotes the OE regeneration.

Previous studies including those from Schwob's lab found that Notch-mediated downregulation of p63 is necessary and sufficient for the activation of HBCs and promotion of OE regeneration (Herrick et al., 2017, 2018; Packard et al., 2011). Interestingly, some studies about crosstalk between p63 and the Hippo/YAP pathway were recently published (Saladi et al., 2017). In different subsets of head and neck squamous cell carcinomas, YAP has been shown to be alternatively dysregulated by Akt phosphorylation and cytoplasmic sequestration or through transcriptional repression by ΔNp63. Dysregulation of YAP, in turn, promoted cell proliferation and migration (Ehsanian et al., 2010). On the other hand, YAP can also positively regulate p63 in airway epithelial cells to tune airway epithelial size and architecture (Zhao et al., 2014). Interestingly, some studies have reported that YAP represses ΔNp63 through ZEB2 to inhibit squamous cells *trans*-differentiation in Lkb1-deficient lung adenocarcinoma (Gao et al., 2014). These previous results indicate that YAP might act as a negative upstream regulator of p63, leading to the activation of HBCs, thereby enhancing functional recovery in OE. Nonetheless, the specific regulatory mechanisms need to be explored further in future.

This study also sought to elucidate the therapeutic effect of YAP on the functional recovery of the olfactory system. We found that activation of YAP enhanced the proliferation of HBCs and promoted OE regeneration after injury (Figure 7) or in AD model mice (Figure S5). Recent studies have shown that Aβ appears in OE at 1–2 months of age, coinciding with the rapid decrease in OE thickness and degeneration of OSNs in both AD model mice and patients (Kovács et al., 1999; Yoo et al., 2017). Therefore, these data indicate that AD model mice suffer from chronic OE injury that leads to olfactory dysfunction and might be considered as a special kind of disease model for chronic OE injury. In summary, YAP may be a potential novel therapeutic target for the management of olfactory dysfunction caused by acute or chronic OE injury.

## EXPERIMENTAL PROCEDURES

### Mouse breeding and genotyping

$YAP^{K5}$-CKO mice were obtained by crossing the floxed YAP allele ($YAP^{f/f}$) with K5-Cre transgenic mice (gifted from Prof. Xiao Yang's lab, Chinese Academy of Military Science, Beijing, China) (Yan et al., 2015). AD model mice (APP/PS1 mice) were purchased from Shanghai Model Organisms Center. Animal tests were approved by the Animal Bioethics Committee of Wenzhou Medical University and Hangzhou Normal University.

### The methimazole-induced OE injury model

In brief, methimazole (#301507, Sigma) was dissolved in PBS (10 mg/mL in stock solution) and administered to 2-month-old mice at a dose of 75 mg/kg by intraperitoneal injection. Post-injection care was then provided.

### Injection of drugs and reagents

After methimazole injection, mice were treated with JTE013 (#10009458, Cayman), XMU-MP-1 (HY-100526, MCE), or S1P (HY-108496, MCE). JTE013 was dissolved in PBS containing DMSO (5%) and BSA (3%) before being injected intraperitoneally at a dose of 3 mg/kg per day after injury (Japtok et al., 2015). XMU-MP-1 was dissolved in DMSO and injected intraperitoneally at a dose of 1 mg/kg, given every 2 days after injury (Xie et al., 2020). S1P was dissolved in 0.001% BSA and injected subcutaneously at a dose of 1 mg/mL, given every 7 days after injury (Roviezzo et al., 2015).

### Behavioral test and analysis

In brief, cookies were put in cages 3 days before testing. In addition, mice were subjected to a fast for 18–20 h with water as the only provision, and transferred into the cages followed by acclimation for 5 min in a quiet and gloomy environment. A piece of cookie was

buried 2.3–2.5 cm below the surface of a 3-cm-deep layer of clean bedding material, and the location of the food pellet was changed regularly in a random pattern. The mice were considered to have successfully completed the task after grasping the buried food with their forepaws and/or teeth. The time of completion was defined as the duration within which a mouse found the food after being transferred into the cage. Subjects that failed to find the food particles within 5 min were considered to have abnormal olfactory function.

### Western blotting

OE tissues were lysed in lysis buffer for 30 min on ice. The lysis buffer consisted of 50 mM Tris-HCl (pH 7.4), 150 mM NaCl, 1% NP-40, 0.5% Triton X-100, 5 mM sodium fluoride, 1 mM EDTA, 1 mM phenylmethylsulfonylfluoride, 2 mM sodium orthovanadate, and a protease inhibitor cocktail (P8340, Sigma). The lysates were then centrifuged at 12,000 rpm for 30 min to obtain the suspended proteins. The proteins were extracted after adding 5× loading buffer and denatured at 100°C for 10 min before being separated by SDS-PAGE (8%–12%). The proteins were then transferred into nitrocellulose membranes (Life Sciences) and immersed in 5% skim milk for blocking at room temperature for 1 h, followed by an overnight incubation with primary antibodies at 4°C, then rinsed with Tris-buffered saline with Tween 20 and incubated for 1 h at room temperature after adding the appropriate secondary antibodies (1:5,000, Bio-Rad). Primary antibodies included anti-p-YAP (Ser127, 1:1,000, #4911, CST), anti-YAP (1:1,000, ab205270, Abcam), anti-TAZ (1:1,000, DF4653, Affinity), anti-MOB1 (1:1,000, #13730, CST), and anti-p-MOB1 (Thr35, 1:1,000, #8699, CST). Anti-GAPDH (1:5,000, #2118, CST) and anti-β-actin (1:10,000, A5316, Sigma) were used as loading controls. Protein bands were detected through ECL (Bio-Rad), and analyzed by Quantity One software (Bio-Rad).

### Immunostaining

After perfusion with 0.1 M PBS followed by 4% PFA, the OE tissues were fixed with fresh 4% PFA after which they were decalcified using 10% EDTA in PBS at 4°C for 5 days. All tissues were also dehydrated using 30% sucrose in PBS until they sank. The OE tissues were then sectioned in 20-μm-thick sections. Sections were washed three times with PBS and fixed with fresh 4% PFA for 30 min. The antigens were repaired for 30 min at 90°C using sodium citrate antigen retrieval solution (Solarbio). The tissue sections were immersed in 0.3% Triton X-100 and 5% BSA for blocking at room temperature and processed by incubation with primary antibodies at 4°C overnight (Ho et al., 2019; Inokuchi et al., 2017; Ito-Ishida et al., 2018; Xie et al., 2020). Primary antibodies included anti-YAP (1:200, WH0010413M1, Sigma), anti-YAP (1:200, ab205270, Abcam), anti-p63 (1:200, CM 163A, Biocare Medical), anti-p63 (1:200, sc-25268, Santa Cruz Biotechnology), anti-K5 (1:200, ab52635, Abcam), anti-GAP43 (1:500, ab16053, Abcam), anti-OMP (1:500, #544-10001, Wako), anti-S1PR1 (1:200, ab23695, Abcam), anti-S1PR2 (1:200, 21180-AP, Proteintech), anti-Ki67 (1:300, AB9260, Millipore), anti-Ki67 (1:200, ab16667, Abcam), anti-PH3 (1:500, ab14955, Abcam), anti-Sox9 (1:500, ab185966, Abcam), and anti-LSD1 (1:200, ab17721, Abcam). The sections were washed three times with PBS and incubated with the corresponding secondary antibodies (1:1,000, Invitrogen) for 1 h. Images were acquired by a SLIDEVIEW VS200 microscope (Olympus, Germany) and confocal microscopes (Nikon, Japan), and analyzed by Image J or Adobe Photoshop CC 14.0 software.

### Statistical analysis

All the data presented represent results from at least three independent experiments. GraphPad Prism software was used for statistical analysis, and Student's t test, one-way ANOVA, or two-way ANOVA were utilized. Statistical significance was defined as $p < 0.05$.

## SUPPLEMENTAL INFORMATION

Supplemental information can be found online at https://doi.org/10.1016/j.stemcr.2022.01.007.

## AUTHOR CONTRIBUTIONS

Z.H., Y.W., and X.X. contributed to the conception and design of the study. Q.W. and X.M. carried out most of the western blot and immunofluorescent staining experiments. Q.W., X.B., W.W., L.X., X.S., X.W., D.Y., S.D., and J.Z. contributed to the acquisition and interpretation of the data and organized the pictures. Y.F., S.X., Z.C., X.L., Y.L., F.L., and S.L. helped to breed mice and did genotyping. Q.W. wrote the manuscript. X.X., Y.W., H.T., and Z.H. contributed to revising the original text and provided the funding. All authors approved the final version of the manuscript.

## CONFLICTS OF INTEREST

The authors declare no competing interests.

## ACKNOWLEDGMENTS

This work was supported by the Natural Science Foundation of Zhejiang Province (LR18C090001, LQ21C090009), National Natural Science Foundation (92049104, 81771348, 81971172), Planted Talent Plan Projects for College Students in Zhejiang Province (2019 R413078 and 2020R413077), National College Students' Innovation and Entrepreneurship Training Program (201910343027), Basic Scientific Research Project of Wenzhou (Y2020241).

Received: December 16, 2020
Revised: January 7, 2022
Accepted: January 10, 2022
Published: February 10, 2022

## REFERENCES

Akladios, B., Mendoza-Reinoso, V., Samuel, M.S., Hardeman, E.C., Khosrotehrani, K., Key, B., and Beverdam, A. (2017). Epidermal YAP2-5SA-ΔC drives β-catenin activation to promote keratinocyte proliferation in mouse skin in vivo. J. Invest. Dermatol. *137*, 716–726. https://doi.org/10.1016/j.jid.2016.10.029.

Andl, T., Zhou, L., Yang, K., Kadekaro, A.L., and Zhang, Y. (2017). YAP and WWTR1: new targets for skin cancer treatment. Cancer Lett. *396*, 30–41. https://doi.org/10.1016/j.canlet.2017.03.001.

Attems, J., Walker, L., and Jellinger, K.A. (2015). Olfaction and aging: a mini-review. Gerontology *61*, 485–490. https://doi.org/10.1159/000381619.

Azzolin, L., Panciera, T., Soligo, S., Enzo, E., Bicciato, S., Dupont, S., Bresolin, S., Frasson, C., Basso, G., Guzzardo, V., et al. (2014). YAP/TAZ incorporation in the β-catenin destruction complex orchestrates the Wnt response. Cell *158*, 157–170. https://doi.org/10.1016/j.cell.2014.06.013.

Bahar-Fuchs, A., Chételat, G., Villemagne, V.L., Moss, S., Pike, K., Masters, C.L., Rowe, C., and Savage, G. (2010). Olfactory deficits and amyloid-β burden in Alzheimer's disease, mild cognitive impairment, and healthy aging: a PiB PET study. J. Alzheimers Dis. *22*, 1081–1087. https://doi.org/10.3233/jad-2010-100696.

Bao, X., Xu, X., Wu, Q., Zhang, J., Feng, W., Yang, D., Li, F., Lu, S., Liu, H., Shen, X., et al. (2020). Sphingosine 1-phosphate promotes the proliferation of olfactory ensheathing cells through YAP signaling and participates in the formation of olfactory nerve layer. Glia *68*, 1757–1774. https://doi.org/10.1002/glia.23803.

Carter, L.A., MacDonald, J.L., and Roskams, A.J. (2004). Olfactory horizontal basal cells demonstrate a conserved multipotent progenitor phenotype. J. Neurosci. *24*, 5670–5683. https://doi.org/10.1523/jneurosci.0330-04.2004.

Chen, M., Reed, R.R., and Lane, A.P. (2017). Acute inflammation regulates neuroregeneration through the NF-κB pathway in olfactory epithelium. Proc. Natl. Acad. Sci. U S A *114*, 8089–8094. https://doi.org/10.1073/pnas.1620664114.

Chen, M., Reed, R.R., and Lane, A.P. (2019). Chronic inflammation directs an olfactory stem cell functional switch from neuroregeneration to immune defense. Cell Stem Cell *25*, 501–513.e5. https://doi.org/10.1016/j.stem.2019.08.011.

Chen, M., Tian, S., Yang, X., Lane, A.P., Reed, R.R., and Liu, H. (2014). Wnt-responsive Lgr5$^+$ globose basal cells function as multipotent olfactory epithelium progenitor cells. J. Neurosci. *34*, 8268–8276. https://doi.org/10.1523/jneurosci.0240-14.2014.

Cheng, J.C., Wang, E.Y., Yi, Y., Thakur, A., Tsai, S.H., and Hoodless, P.A. (2018). S1P stimulates proliferation by upregulating CTGF expression through S1PR2-mediated YAP activation. Mol. Cancer Res. *16*, 1543–1555. https://doi.org/10.1158/1541-7786.mcr-17-0681.

Choi, R., and Goldstein, B.J. (2018). Olfactory epithelium: cells, clinical disorders, and insights from an adult stem cell niche. Laryngoscope Investig. Otolaryngol. *3*, 35–42. https://doi.org/10.1002/lio2.135.

Doty, R.L. (2018). Age-related deficits in taste and smell. Otolaryngol. Clin. North Am. *51*, 815–825. https://doi.org/10.1016/j.otc.2018.03.014.

Ehsanian, R., Brown, M., Lu, H., Yang, X.P., Pattatheyil, A., Yan, B., Duggal, P., Chuang, R., Doondeea, J., Feller, S., et al. (2010). YAP dysregulation by phosphorylation or ΔNp63-mediated gene repression promotes proliferation, survival and migration in head and neck cancer subsets. Oncogene *29*, 6160–6171. https://doi.org/10.1038/onc.2010.339.

Elbediwy, A., and Thompson, B.J. (2018). Evolution of mechanotransduction via YAP/TAZ in animal epithelia. Curr. Opin. Cell Biol. *51*, 117–123. https://doi.org/10.1016/j.ceb.2018.02.003.

Elbediwy, A., Vincent-Mistiaen, Z.I., Spencer-Dene, B., Stone, R.K., Boeing, S., Wculek, S.K., Cordero, J., Tan, E.H., Ridgway, R., Brunton, V.G., et al. (2016). Integrin signalling regulates YAP and TAZ to control skin homeostasis. Development *143*, 1674–1687. https://doi.org/10.1242/dev.133728.

Fletcher, R.B., Das, D., Gadye, L., Street, K.N., Baudhuin, A., Wagner, A., Cole, M.B., Flores, Q., Choi, Y.G., Yosef, N., et al. (2017). Deconstructing olfactory stem cell trajectories at single-cell resolution. Cell Stem Cell *20*, 817–830.e8. https://doi.org/10.1016/j.stem.2017.04.003.

Fletcher, R.B., Prasol, M.S., Estrada, J., Baudhuin, A., Vranizan, K., Choi, Y.G., and Ngai, J. (2011). p63 regulates olfactory stem cell self-renewal and differentiation. Neuron *72*, 748–759. https://doi.org/10.1016/j.neuron.2011.09.009.

Gao, Y., Zhang, W., Han, X., Li, F., Wang, X., Wang, R., Fang, Z., Tong, X., Yao, S., Li, F., et al. (2014). YAP inhibits squamous transdifferentiation of Lkb1-deficient lung adenocarcinoma through ZEB2-dependent DNp63 repression. Nat. Commun. *5*, 4629. https://doi.org/10.1038/ncomms5629.

Gregorieff, A., Liu, Y., Inanlou, M.R., Khomchuk, Y., and Wrana, J.L. (2015). Yap-dependent reprogramming of Lgr5(+) stem cells drives intestinal regeneration and cancer. Nature *526*, 715–718. https://doi.org/10.1038/nature15382.

Hageman, J.H., Heinz, M.C., Kretzschmar, K., van der Vaart, J., Clevers, H., and Snippert, H.J.G. (2020). Intestinal regeneration: regulation by the microenvironment. Dev. Cell *54*, 435–446. https://doi.org/10.1016/j.devcel.2020.07.009.

Herrick, D.B., Guo, Z., Jang, W., Schnittke, N., and Schwob, J.E. (2018). Canonical notch signaling directs the fate of differentiating neurocompetent progenitors in the mammalian olfactory epithelium. J. Neurosci. *38*, 5022–5037. https://doi.org/10.1523/jneurosci.0484-17.2018.

Herrick, D.B., Lin, B., Peterson, J., Schnittke, N., and Schwob, J.E. (2017). Notch1 maintains dormancy of olfactory horizontal basal cells, a reserve neural stem cell. Proc. Natl. Acad. Sci. U S A *114*, E5589–E5598. https://doi.org/10.1073/pnas.1701333114.

Ho, I.H.T., Liu, X., Zou, Y., Liu, T., Hu, W., Chan, H., Tian, Y., Zhang, Y., Li, Q., Kou, S., et al. (2019). A novel peptide interfering with proBDNF-sortilin interaction alleviates chronic inflammatory pain. Theranostics *9*, 1651–1665. https://doi.org/10.7150/thno.29703.

Holbrook, E.H., Szumowski, K.E., and Schwob, J.E. (1995). An immunochemical, ultrastructural, and developmental characterization of the horizontal basal cells of rat olfactory epithelium. J. Comp. Neurol. *363*, 129–146. https://doi.org/10.1002/cne.903630111.

Huang, Z., Hu, J., Pan, J., Wang, Y., Hu, G., Zhou, J., Mei, L., and Xiong, W.C. (2016). YAP stabilizes SMAD1 and promotes BMP2-induced neocortical astrocytic differentiation. Development *143*, 2398–2409. https://doi.org/10.1242/dev.130658.

Huard, J.M., and Schwob, J.E. (1995). Cell cycle of globose basal cells in rat olfactory epithelium. Dev. Dyn. *203*, 17–26. https://doi.org/10.1002/aja.1002030103.

Inokuchi, K., Imamura, F., Takeuchi, H., Kim, R., Okuno, H., Nishizumi, H., Bito, H., Kikusui, T., and Sakano, H. (2017). Nrp2 is sufficient to instruct circuit formation of mitral-cells to mediate odour-induced attractive social responses. Nat. Commun. *8*, 15977. https://doi.org/10.1038/ncomms15977.

Ito-Ishida, A., Yamalanchili, H.K., Shao, Y., Baker, S.A., Heckman, L.D., Lavery, L.A., Kim, J.Y., Lombardi, L.M., Sun, Y., Liu, Z., et al. (2018). Genome-wide distribution of linker histone H1.0 is independent of MeCP2. Nat. Neurosci. *21*, 794–798. https://doi.org/10.1038/s41593-018-0155-8.

Iwai, N., Zhou, Z., Roop, D.R., and Behringer, R.R. (2008). Horizontal basal cells are multipotent progenitors in normal and injured adult olfactory epithelium. Stem Cells *26*, 1298–1306. https://doi.org/10.1634/stemcells.2007-0891.

Japtok, L., Schmitz, E.I., Fayyaz, S., Krämer, S., Hsu, L.J., and Kleuser, B. (2015). Sphingosine 1-phosphate counteracts insulin signaling in pancreatic β-cells via the sphingosine 1-phosphate receptor subtype 2. Faseb J *29*, 3357–3369. https://doi.org/10.1096/fj.14-263194.

Joiner, A.M., Green, W.W., McIntyre, J.C., Allen, B.L., Schwob, J.E., and Martens, J.R. (2015). Primary cilia on horizontal basal cells regulate regeneration of the olfactory epithelium. J. Neurosci. *35*, 13761–13772. https://doi.org/10.1523/jneurosci.1708-15.2015.

Kikuta, S., Sakamoto, T., Nagayama, S., Kanaya, K., Kinoshita, M., Kondo, K., Tsunoda, K., Mori, K., and Yamasoba, T. (2015). Sensory deprivation disrupts homeostatic regeneration of newly generated olfactory sensory neurons after injury in adult mice. J. Neurosci. *35*, 2657–2673. https://doi.org/10.1523/jneurosci.2484-14.2015.

Kovács, T., Cairns, N.J., and Lantos, P.L. (1999). beta-amyloid deposition and neurofibrillary tangle formation in the olfactory bulb in ageing and Alzheimer's disease. Neuropathol. Appl. Neurobiol. *25*, 481–491. https://doi.org/10.1046/j.1365-2990.1999.00208.x.

Lee, M.J., Byun, M.R., Furutani-Seiki, M., Hong, J.H., and Jung, H.S. (2014). YAP and TAZ regulate skin wound healing. J. Invest. Dermatol. *134*, 518–525. https://doi.org/10.1038/jid.2013.339.

Leung, C.T., Coulombe, P.A., and Reed, R.R. (2007). Contribution of olfactory neural stem cells to tissue maintenance and regeneration. Nat. Neurosci. *10*, 720–726. https://doi.org/10.1038/nn1882.

Lian, I., Kim, J., Okazawa, H., Zhao, J., Zhao, B., Yu, J., Chinnaiyan, A., Israel, M.A., Goldstein, L.S., Abujarour, R., et al. (2010). The role of YAP transcription coactivator in regulating stem cell self-renewal and differentiation. Genes Dev. *24*, 1106–1118. https://doi.org/10.1101/gad.1903310.

Liu, L., Zhai, C., Pan, Y., Zhu, Y., Shi, W., Wang, J., Yan, X., Su, X., Song, Y., Gao, L., et al. (2018). Sphingosine-1-phosphate induces airway smooth muscle cell proliferation, migration, and contraction by modulating Hippo signaling effector YAP. Am. J. Physiol. Lung Cell Mol. Physiol. *315*, L609–L621. https://doi.org/10.1152/ajplung.00554.2017.

Mendoza-Reinoso, V., and Beverdam, A. (2018). Epidermal YAP activity drives canonical WNT16/β-catenin signaling to promote keratinocyte proliferation in vitro and in the murine skin. Stem Cell Res. *29*, 15–23. https://doi.org/10.1016/j.scr.2018.03.005.

Moya, I.M., and Halder, G. (2019). Hippo-YAP/TAZ signalling in organ regeneration and regenerative medicine. Nat. Rev. Mol. Cell Biol. *20*, 211–226. https://doi.org/10.1038/s41580-018-0086-y.

Ogawa, T., Takezawa, K., Shimizu, S., and Shimizu, T. (2014). Valproic acid promotes neural regeneration of olfactory epithelium in adult mice after methimazole-induced damage. Am. J. Rhinol. Allergy *28*, e95–e99. https://doi.org/10.2500/ajra.2014.28.4027.

Packard, A., Schnittke, N., Romano, R.A., Sinha, S., and Schwob, J.E. (2011). DeltaNp63 regulates stem cell dynamics in the mammalian olfactory epithelium. J. Neurosci. *31*, 8748–8759. https://doi.org/10.1523/jneurosci.0681-11.2011.

Peterson, J., Lin, B., Barrios-Camacho, C.M., Herrick, D.B., Holbrook, E.H., Jang, W., Coleman, J.H., and Schwob, J.E. (2019). Activating a reserve neural stem cell population in vitro enables engraftment and multipotency after transplantation. Stem Cell Rep. *12*, 680–695. https://doi.org/10.1016/j.stemcr.2019.02.014.

Rognoni, E., and Walko, G. (2019). The roles of YAP/TAZ and the Hippo pathway in healthy and diseased skin. Cells *8*, 411. https://doi.org/10.3390/cells8050411.

Roviezzo, F., Sorrentino, R., Bertolino, A., De Gruttola, L., Terlizzi, M., Pinto, A., Napolitano, M., Castello, G., D'Agostino, B., Ianaro, A., et al. (2015). S1P-induced airway smooth muscle hyperresponsiveness and lung inflammation in vivo: molecular and cellular mechanisms. Br. J. Pharmacol. *172*, 1882–1893. https://doi.org/10.1111/bph.13033.

Saladi, S.V., Ross, K., Karaayvaz, M., Tata, P.R., Mou, H., Rajagopal, J., Ramaswamy, S., and Ellisen, L.W. (2017). ACTL6A is co-amplified with p63 in squamous cell carcinoma to drive YAP activation, regenerative proliferation, and poor prognosis. Cancer Cell *31*, 35–49. https://doi.org/10.1016/j.ccell.2016.12.001.

Schlegelmilch, K., Mohseni, M., Kirak, O., Pruszak, J., Rodriguez, J.R., Zhou, D., Kreger, B.T., Vasioukhin, V., Avruch, J., Brummelkamp, T.R., et al. (2011). Yap1 acts downstream of α-catenin to control epidermal proliferation. Cell *144*, 782–795. https://doi.org/10.1016/j.cell.2011.02.031.

Schnittke, N., Herrick, D.B., Lin, B., Peterson, J., Coleman, J.H., Packard, A.I., Jang, W., and Schwob, J.E. (2015). Transcription factor p63 controls the reserve status but not the stemness of horizontal basal cells in the olfactory epithelium. Proc. Natl. Acad. Sci. U S A *112*, E5068–E5077. https://doi.org/10.1073/pnas.1512272112.

Schwob, J.E., Jang, W., Holbrook, E.H., Lin, B., Herrick, D.B., Peterson, J.N., and Hewitt Coleman, J. (2017). Stem and progenitor cells of the mammalian olfactory epithelium: taking poietic license. J. Comp. Neurol. *525*, 1034–1054. https://doi.org/10.1002/cne.24105.

Schwob, J.E., Youngentob, S.L., and Mezza, R.C. (1995). Reconstitution of the rat olfactory epithelium after methyl bromide-induced lesion. J. Comp. Neurol. *359*, 15–37. https://doi.org/10.1002/cne.903590103.

Taniguchi, K., Wu, L.W., Grivennikov, S.I., de Jong, P.R., Lian, I., Yu, F.X., Wang, K., Ho, S.B., Boland, B.S., Chang, J.T., et al. (2015). A gp130-Src-YAP module links inflammation to epithelial regeneration. Nature *519*, 57–62. https://doi.org/10.1038/nature14228.

Tukijan, F., Chandrakanthan, M., and Nguyen, L.N. (2018). The signalling roles of sphingosine-1-phosphate derived from red blood cells and platelets. Br. J. Pharmacol. *175*, 3741–3746. https://doi.org/10.1111/bph.14451.

Wu, N., Rao, X., Gao, Y., Wang, J., and Xu, F. (2013). Amyloid-β deposition and olfactory dysfunction in an Alzheimer's disease model. J. Alzheimers Dis. *37*, 699–712. https://doi.org/10.3233/jad-122443.

Xie, C., Shen, X., Xu, X., Liu, H., Li, F., Lu, S., Gao, Z., Zhang, J., Wu, Q., Yang, D., et al. (2020). Astrocytic YAP promotes the formation of glia scars and neural regeneration after spinal cord injury. J. Neurosci. *40*, 2644–2662. https://doi.org/10.1523/jneurosci.2229-19.2020.

Yan, S., Xu, Z., Lou, F., Zhang, L., Ke, F., Bai, J., Liu, Z., Liu, J., Wang, H., Zhu, H., et al. (2015). NF-κB-induced microRNA-31 promotes epidermal hyperplasia by repressing protein phosphatase 6 in psoriasis. Nat. Commun. *6*, 7652. https://doi.org/10.1038/ncomms8652.

Yao, M., Wang, Y., Zhang, P., Chen, H., Xu, Z., Jiao, J., and Yuan, Z. (2014). BMP2-SMAD signaling represses the proliferation of embryonic neural stem cells through YAP. J. Neurosci. *34*, 12039–12048. https://doi.org/10.1523/jneurosci.0486-14.2014.

Yoo, S.J., Lee, J.H., Kim, S.Y., Son, G., Kim, J.Y., Cho, B., Yu, S.W., Chang, K.A., Suh, Y.H., and Moon, C. (2017). Differential spatial expression of peripheral olfactory neuron-derived BACE1 induces olfactory impairment by region-specific accumulation of β-amyloid oligomer. Cell Death Dis. *8*, e2977. https://doi.org/10.1038/cddis.2017.349.

Yu, F.X., Zhao, B., Panupinthu, N., Jewell, J.L., Lian, I., Wang, L.H., Zhao, J., Yuan, H., Tumaneng, K., Li, H., et al. (2012). Regulation of the Hippo-YAP pathway by G-protein-coupled receptor signaling. Cell *150*, 780–791. https://doi.org/10.1016/j.cell.2012.06.037.

Yu, O.M., Miyamoto, S., and Brown, J.H. (2016). Myocardin-related transcription factor A and yes-associated protein exert dual control in G protein-coupled receptor- and RhoA-mediated transcriptional regulation and cell proliferation. Mol. Cell Biol. *36*, 39–49. https://doi.org/10.1128/mcb.00772-15.

Zhang, A.J., Lee, A.C., Chu, H., Chan, J.F., Fan, Z., Li, C., Liu, F., Chen, Y., Yuan, S., Poon, V.K., et al. (2021). Severe acute respiratory syndrome coronavirus 2 infects and damages the mature and immature olfactory sensory neurons of hamsters. Clin. Infect. Dis. *73*, e503–e512. https://doi.org/10.1093/cid/ciaa995.

Zhang, W., Nandakumar, N., Shi, Y., Manzano, M., Smith, A., Graham, G., Gupta, S., Vietsch, E.E., Laughlin, S.Z., Wadhwa, M., et al. (2014). Downstream of mutant KRAS, the transcription regulator YAP is essential for neoplastic progression to pancreatic ductal adenocarcinoma. Sci. Signal *7*, ra42. https://doi.org/10.1126/scisignal.2005049.

Zhao, R., Fallon, T.R., Saladi, S.V., Pardo-Saganta, A., Villoria, J., Mou, H., Vinarsky, V., Gonzalez-Celeiro, M., Nunna, N., Hariri, L.P., et al. (2014). Yap tunes airway epithelial size and architecture by regulating the identity, maintenance, and self-renewal of stem cells. Dev. Cell *30*, 151–165. https://doi.org/10.1016/j.devcel.2014.06.004.

**Stem Cell Reports, Volume *17***

## Supplemental Information

# YAP signaling in horizontal basal cells promotes the regeneration of olfactory epithelium after injury

**Qian Wu, Xingxing Xu, Xuemeng Miao, Xiaomei Bao, Xiuchun Li, Ludan Xiang, Wei Wang, Siyu Du, Yi Lu, Xiwu Wang, Danlu Yang, Jingjing Zhang, Xiya Shen, Fayi Li, Sheng Lu, Yiren Fan, Shujie Xu, Zihao Chen, Ying Wang, Honglin Teng, and Zhihui Huang**

**Supplemental Information**

**Supplemental Figures and legends**

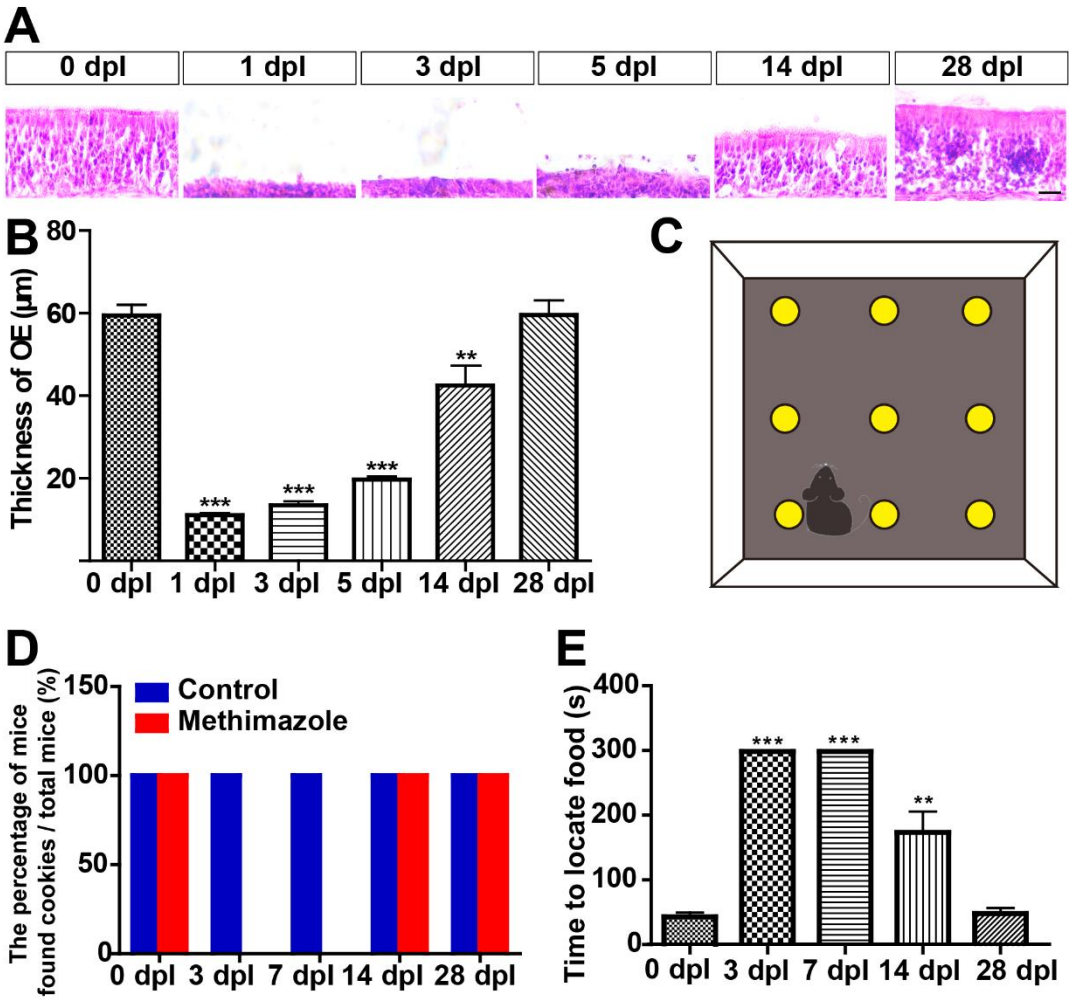


**Figure S1. Establishment of methimazole-induced OE injury model.**

(A) HE staining in the OE of 2 months old C57BL/6 mice at 0, 1, 3, 5, 14 and 28 dpl. (B) Quantitative analysis of the thickness of 2 months old OE as shown in (A) (n = 10 sections from 5 mice per group). (C) The schematic diagram of buried pellet test. (D) The percentage of control- or methimazole-treated 2 months old C57BL/6 mice that found cookies over total observed mice at 0, 3, 7, 14 and 28 dpl (n = 13 mice per group, two-way ANOVA with Bonferroni's post-tests, compared with control group). (E) Quantitative analysis of the time to locate food in the buried pellet test at 0, 3, 7, 14 and 28 dpl (n = 13 mice per group). Data were mean ± SEM, one-way ANOVA with Bonferroni's post-tests unless otherwise indicated, compared with 0 dpl, $^{**}P < 0.01$, $^{***}P < 0.001$. Scale bars, 20 μm.

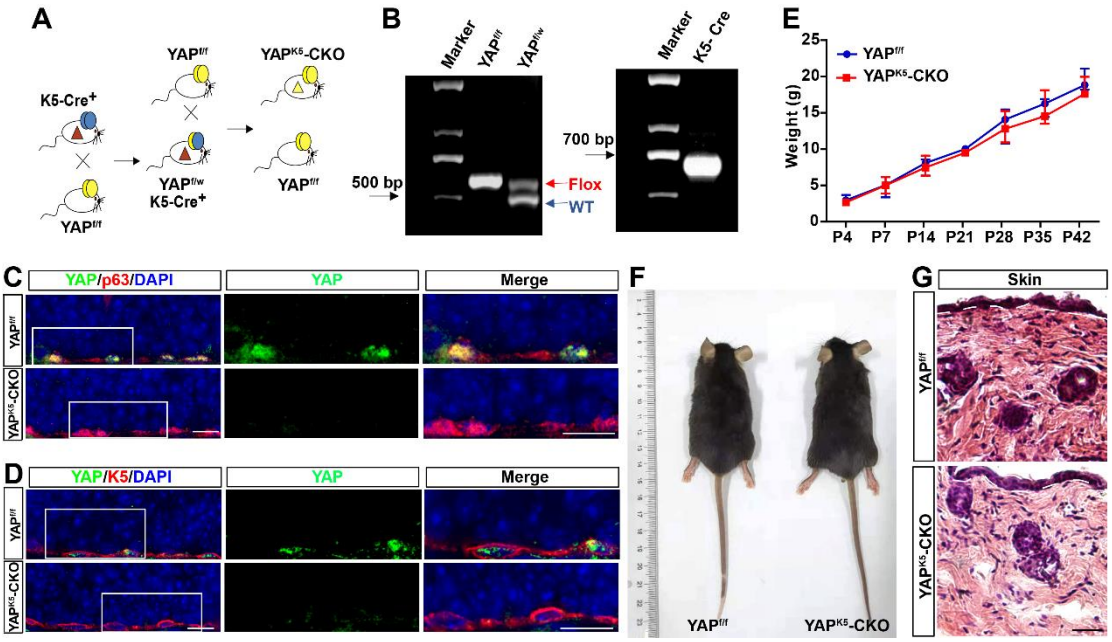


**Figure S2. Identification of YAP$^{K5}$-CKO mice and normal development of skin and hair in YAP$^{K5}$-CKO mice, related to Figures 2, 3, 4.**

(A) The flow chart showed the process of obtaining YAP$^{K5}$-CKO mice and their littermate control. (B) Genotyping was conducted by agarose gel electrophoresis (YAP$^{f/f}$ and YAP$^{f/w}$ mice were shown in the left panel, and K5-Cre mice were shown in the right panel). (C-D) Double immunostaining of YAP (green) and p63 (red) (C), and YAP (green) and K5 (red) (D) in OE of 2 months old YAP$^{f/f}$ and YAP$^{K5}$-CKO mice. (E) Body weight of YAP$^{f/f}$ and YAP$^{K5}$-CKO mice at different developmental stages (n = 10 mice per group). (F) The gross morphologies of skin and hair of 2 months old YAP$^{f/f}$ and YAP$^{K5}$-CKO mice. (G) HE staining of the skin of 2 months old YAP$^{f/f}$ and YAP$^{K5}$-CKO mice. Images of selected regions were shown at higher magnification. Data were mean ± SEM, two-way ANOVA with Bonferroni's post-tests, compared with YAP$^{f/f}$ group. Scale bars, 20 μm.

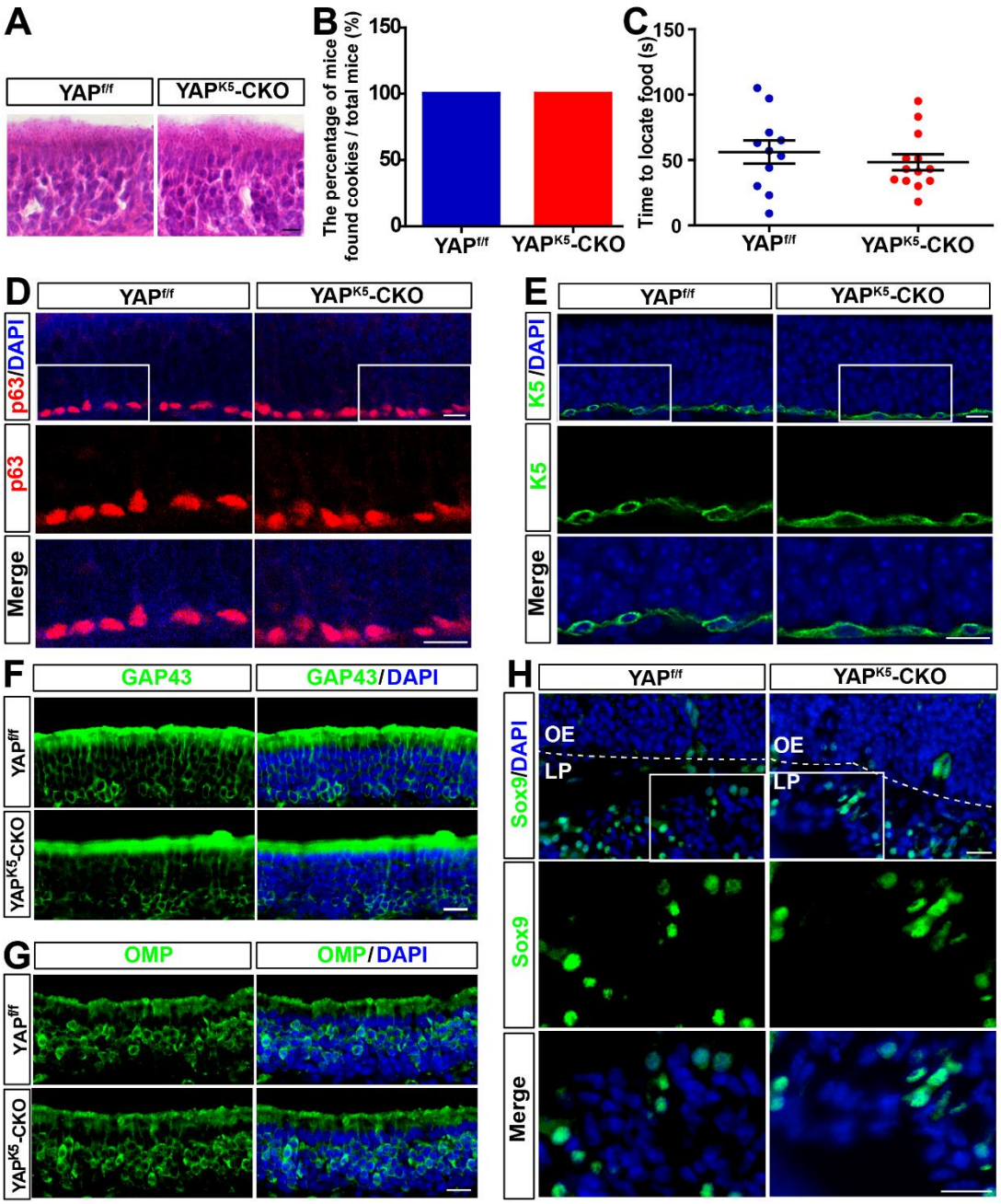


**Figure S3. Normal OE development and olfactory functions of YAP$^{K5}$-CKO mice, related to Figures 2, 3, 4.**

(A) HE staining images of OE from 2 months old YAP$^{f/f}$ and YAP$^{K5}$-CKO mice. (B) The percentage of mice that found cookies over total observed 2 months old YAP$^{f/f}$ (n = 11 mice) or YAP$^{K5}$-CKO mice (n = 13 mice) in the buried pellet test. (C) Quantitative analysis of the time to locate food in the buried pellet test of 2 months old YAP$^{f/f}$ (n = 11 mice) or YAP$^{K5}$-CKO mice (n = 13 mice). (D-H) Immunostaining of p63 (red) (D), K5 (green) (E), GAP43 (green) (F), or OMP (green) (G), or Sox9 (green) (H) in OE of 2 months old YAP$^{f/f}$ and YAP$^{K5}$-CKO mice. Images of selected regions were shown at higher magnification. Data were mean ± SEM, Student's t-test, compared with YAP$^{f/f}$ group. Scale bars, 20 μm.

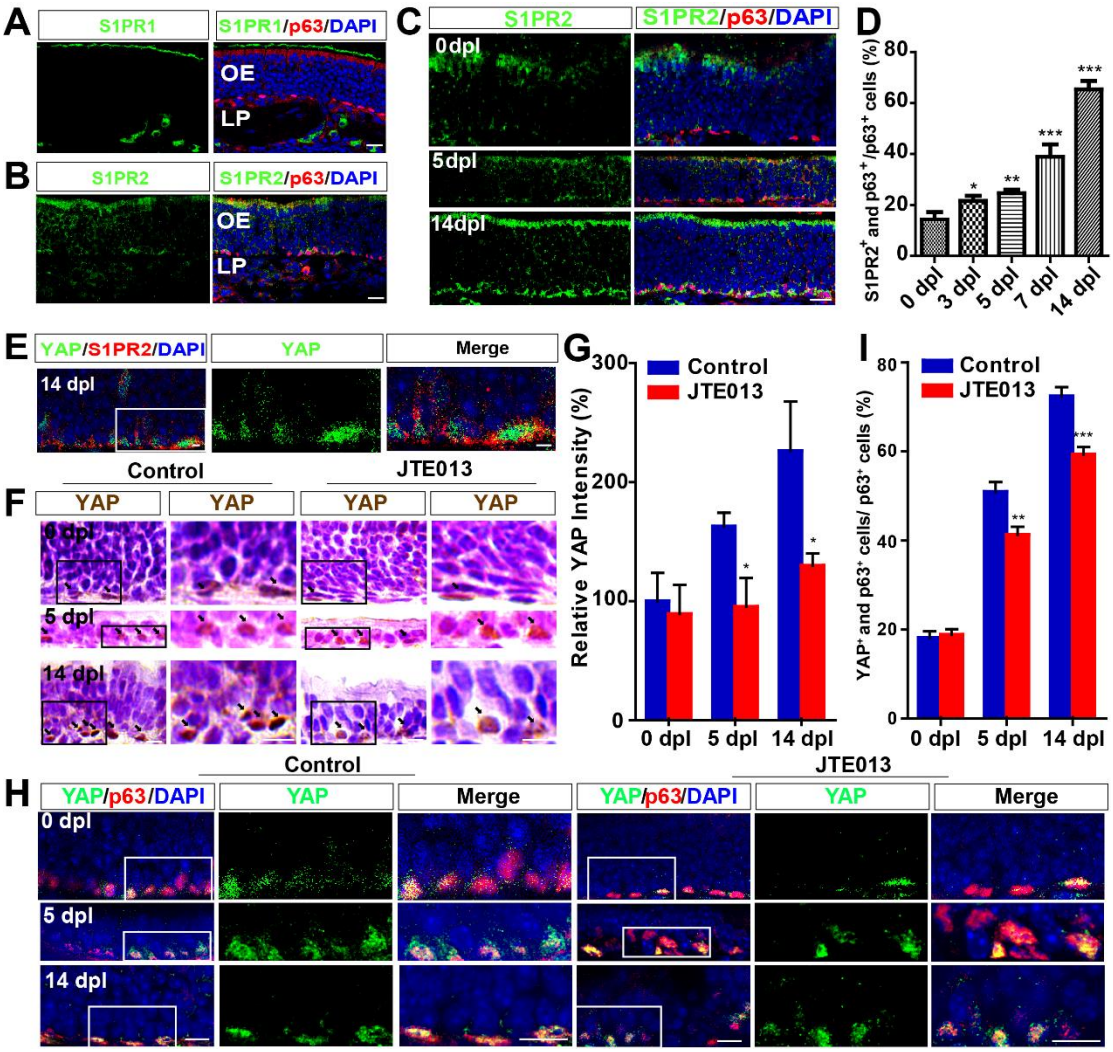


**Figure S4. S1PR2/YAP signaling in HBCs is required for OE regeneration after injury, related to Figures 5, 6.**

(A-B) Double immunostaining of S1PR1 (green) and p63 (red) (A), or S1PR2 (green) and p63 (red) (B) in the OE of 2 months old C57BL/6 mice. (C) Double immunostaining of S1PR2 (green) and p63 (red) in the OE of 2 months old C57BL/6 mice at 0, 5 and 14 dpl. (D) Quantitative analysis of the percentage of cells that showed both S1RP2$^{+}$ and p63$^{+}$ cells over total p63$^{+}$ HBCs at 0, 3, 5, 7 and 14 dpl (n = 8 sections from 4 mice per group) (one-way ANOVA with Bonferroni's post-tests, compared with 0 dpl group). (E) Double immunostaining of YAP (green) and S1PR2 (red) in the OE of 2 months old C57BL/6 mice at 14 dpl. (F) Immunohistochemistry detected the expression of YAP in the OE of control- and JTE013-treated 2 months old C57BL/6 mice at 0, 5 and 14 dpl. (G) Quantitative analysis of the relative YAP density as shown in (F) (n = 6 sections from 3 mice per group). (H) Double immunostaining of YAP (green) and p63 (red) in the OE of control- and JTE013-treated 2 months old C57BL/6 mice at 0, 5 and 14 dpl. (I) Quantitative analysis of the percentage of both YAP$^{+}$ and p63$^{+}$ cells over p63$^{+}$ cells as shown in (H) (n = 5 sections from 3 mice per group). Images of selected regions were shown at higher magnification. Data were mean ± SEM, two-way ANOVA with Bonferroni's post-tests unless otherwise indicated, compared with control group. $^{*}P < 0.05$, $^{**}P < 0.01$, $^{***}P < 0.001$. Scale bars, 20 μm.

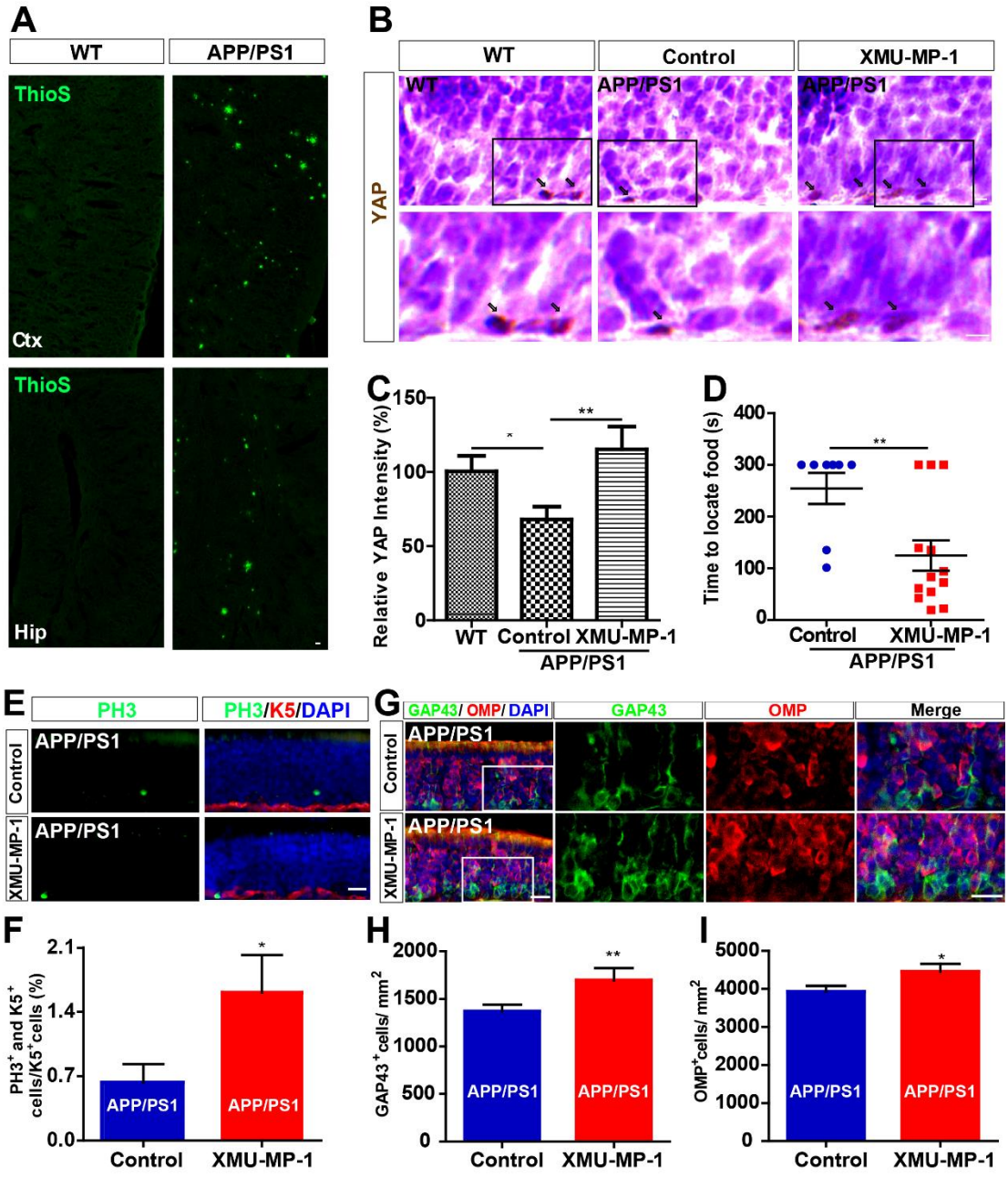


**Figure S5. Activation of YAP signaling by XMU-MP-1 promotes the olfactory functional recovery of AD model mice, related to Figure 7.**

(A) Cortex and hippocampus sections of 9 months old WT and AD model mice were stained with thioflavin-S staining to detect Aβ deposition. Ctx: cortex; Hip: hippocampus. (B) Immunohistochemistry detected the expression of YAP in OE of control-treated 9 months old WT mice, control- and XMU-MP-1-treated 9 months old AD model mice. (C) Quantitative analysis of the relative YAP density as shown in (B) (n = 10 sections from 5 mice per group) (one-way ANOVA with Bonferroni's post-tests, compared with WT group). (D) Quantitative analysis of the time to locate food in control- (n = 8 mice) and XMU-MP-1-treated 9 months old AD model mice (n = 13 mice) in the buried pellet assays. (E) Double immunostaining of PH3 (green) and K5 (red) in the OE of control- and XMU-MP-1-treated 9 months old AD model mice. (F) Quantitative analysis of the percentage of $PH3^+$ and $K5^+$ cells over total $K5^+$ HBCs as shown

in (E) (n = 11 sections from 5 mice per group). (G) Double immunostaining of GAP43 (green) and OMP (red) in the OE of control- and XMU-MP-1-treated 9 months old AD model mice. (H-I) Quantitative analysis of the density of $GAP43^+$ (H) or $OMP^+$ (I) cells as shown in (G) (n = 11 sections from 5 mice per group). Images of selected regions were shown at higher magnification. Data were mean ± SEM, Student's t-test unless otherwise indicated, compared with control group, $^*P < 0.05$, $^{**}P < 0.01$. Scale bars, 20 μm.

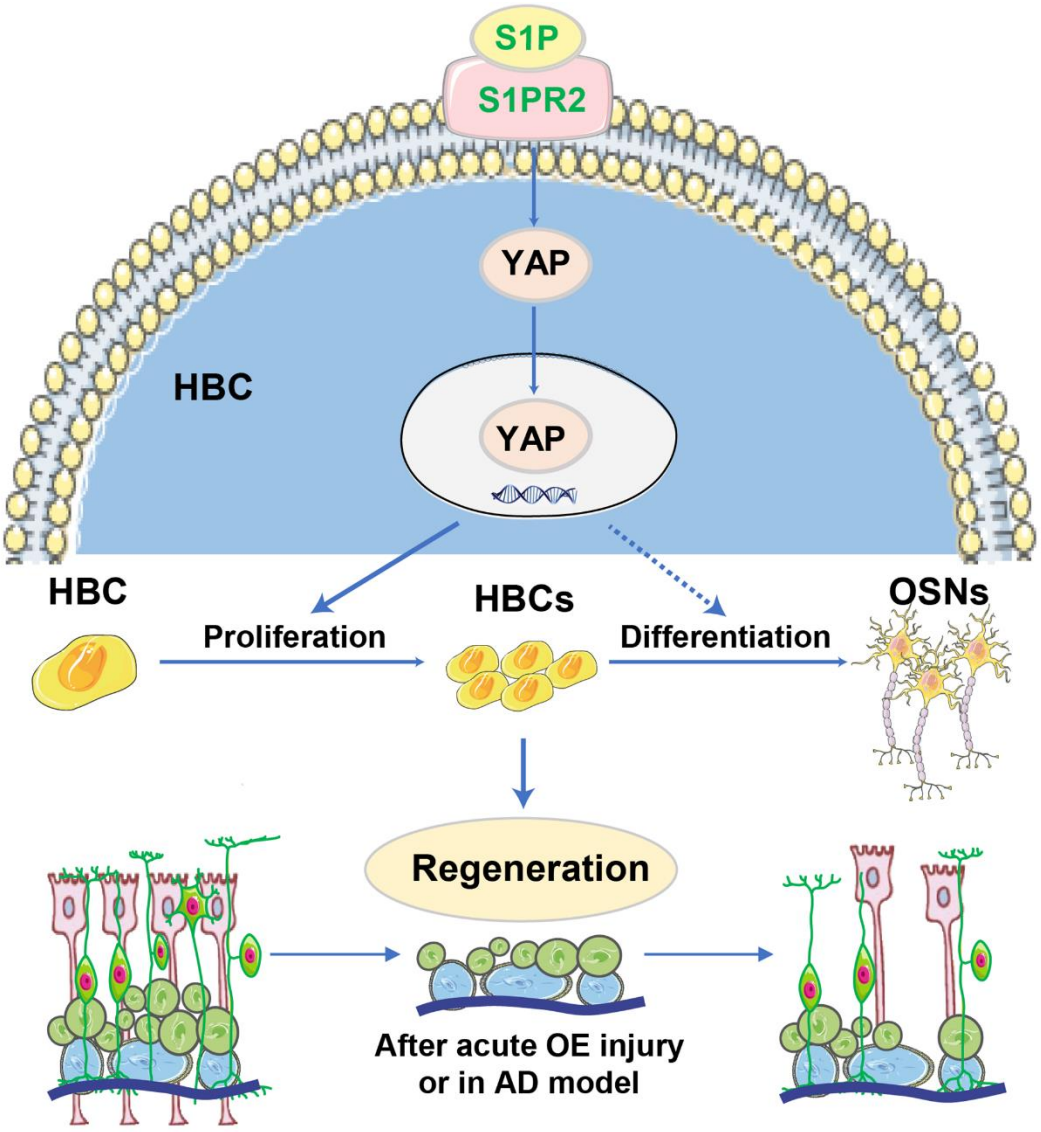


**Figure S6. Working model of YAP's functions in OE regeneration through promoting HBCs proliferation after injury.**

After OE injury, S1P binds to S1PR2 to activate YAP in HBCs, and may trigger OE regeneration through promotion of the proliferation and/ or differentiation of HBCs.

## Supplemental Experimental Procedures

### TUNEL staining

TUNEL staining of the olfactory tissue sections (20 μm in thickness) of 2 months old mice was conducted to evaluate apoptosis. Briefly, the sections were blocked in 5% BSA plus 0.3% Triton X-100 at room temperature for 1 h, after washing with PBS. The *in situ* detection kit was then used according to the manufacturer's protocol (MK500, TaKaRa Bio Inc, Shiga, Japan). The images were acquired through SLIDEVIEW™ VS200 microscope (Olympus, Germany) and analyzed by Image J or Adobe Photoshop CC 14.0 software.

### Hematoxylin-Eosin (HE) staining

Following cardiac perfusion, the tissues were fixed with fresh 4% paraformaldehyde for 1 d, then they were decalcified using 10% EDTA in PBS at 4 °C for 5 d. All tissues were also dehydrated for 3 d using 30% sucrose in PBS until they sank. Thereafter, the olfactory tissues were embedded in optimal cutting temperature before being cut into 20 μm-thick sections, using a freezing microtome (Thermo, USA). The sections were then washed 3 times in double-distilled water after staining with hematoxylin for 4 min. Subsequently, the sections were incubated with acidic liquid alcohol differentiation for 30 s and stained with eosin for 40 s. This was then followed by 95% ethanol, 100% ethanol and a final clearance in xylene before mounting. Images were acquired by SLIDEVIEW™ VS200 microscope (Olympus, Germany) and analyzed by Image J software.

### Thioflavin-S staining

Brain slices (20 μm in thickness) were incubated with 0.1% thioflavin-S (T1892, Sigma, USA) for 8 min at room temperature. The images were acquired through SLIDEVIEW™ VS200 microscope (Olympus, Germany) and analyzed by Image J or Adobe Photoshop CC 14.0 software.

### Immunohistochemistry

Immunohistochemistry of the olfactory tissue sections (20 μm in thickness) of 2 months old mice or 9 months old AD model mice was performed using a kit (SP-9000, Zhong Shan Jin Qiao, China), according to the manufacturer's protocol. Antigen retrieval was accomplished using the sodium citrate antigen retrieval solution at 90°C for 30 min. Thereafter, the endogenous peroxidase activity of the tissue section was blocked with 3% $H_2O_2$ for 0.5 h followed by 5% BSA plus 0.3% Triton X-100 at room temperature for 1 h. After blocking, OE sections were incubated overnight with anti-YAP primary antibody (1:200, ab205270, Abcam) at 4 °C, then washed 3 times with PBS and incubated with a biotin-labeled goat anti-rabbit IgG secondary antibody at room temperature for 20 min. Streptavidin-peroxidase was applied for 20 min at room temperature followed by development with the diaminobenzidine substrate, and then the sections were counterstained with Mayer's Hematoxylin for 2 min. Subsequently, the sections were dehydrated and sealed with neutral gum. The sections were observed under SLIDEVIEW™ VS200 microscope (Olympus, Germany) and brown yellow particles in the nucleus were considered to be YAP positive ($YAP^+$) cells.